Mitral Valve Prostheses

11

Christine Jellis

Mitral valve surgery is one of the most technically demanding aspects of cardiac surgery, owing both to the valve's location and to its complicated structure. Overall cardiac surgical performance is gauged by the rate of successful mitral valve repair. Typically, the best short-term and long-term outcomes are achieved by surgeons who have a subspecialized interest in mitral valve surgery and perform large numbers of repairs in high-volume centers. A repair is usually preferred over a replacement, owing to both longevity and the avoidance of anticoagulation, but repair is not always technically feasible if the valve is stenotic, calcified, significantly thickened, or morphologically unsuitable. A good replacement is always better than a poor repair, which may lead to premature redo surgery. Mitral valve repairs typically involve plication of the posterior leaflet and insertion of an annuloplasty ring. An Alfieri stitch is sometimes included to optimize leaflet coaptation. Mitral valve replacements can be both bioprosthetic and mechanical. Individualized factors including the patient's age, suitability for anticoagulation, and plans for future pregnancies are all important to consider when deciding on the best approach. Robotic mitral valve surgery with femoral cannulation via a mini-thoracotomy is now providing an alternative to traditional approaches via a median sternotomy. Percutaneous valve replacement or repair using various clip devices is now a viable alternative for some patients [*see* Chap. 6]. Valvuloplasty may be adjunctively performed as a temporizing bridge to surgery or a more palliative procedure in the setting of significant mitral stenosis, although factors such as valve and subvalvular thickening and calcification will ultimately govern suitability for this procedure.

Like all surgery, mitral valve surgery can be associated with complications. Echocardiography plays an important role in the perioperative and long-term monitoring of valve function. Transesophageal echocardiography is often useful to overcome issues with poor leaflet visualization and valve shadowing on transthoracic echo. 3D/4D imaging of the mitral valve has revolutionized prosthetic valve assessment by providing better temporal and spatial resolution than traditional 2D imaging (Fig. 11.1). Small paravalvular leaks can be readily identified and localized, thereby allowing better preoperative surgical planning or consideration of percutaneous options. In additional to prosthetic valve degeneration with associated regurgitation or stenosis, other complications include paravalvular leaks due to valve dehiscence and valvular dysfunction due to pannus, inflammatory response, thrombus, or endocarditis.

Video 11.1 A 3D image of a normally functioning, trileaflet, Biocor bioprosthetic mitral valve replacement viewed from the left atrium. High image resolution enables the leaflets, annulus, and even sutures to be clearly demonstrated. The 3D image is conventionally orientated with the aortic valve at the 12 o'clock position, thereby allowing consistency of image description and better ease of interpretation (AVI 1528 kb)

Electronic supplementary material The online version of this chapter (doi:10.1007/978-1-4471-6672-6_11) contains supplementary material, which is available to authorized users.

C. Jellis
Department of Cardiovascular Medicine, Cleveland Clinic,
9500 Euclid Avenue, Cleveland, OH 44195, USA
e-mail: jellisc@ccf.org

M. Desai et al. (eds.), *An Atlas of Mitral Valve Imaging*,
DOI 10.1007/978-1-4471-6672-6_11, © Springer-Verlag London 2015

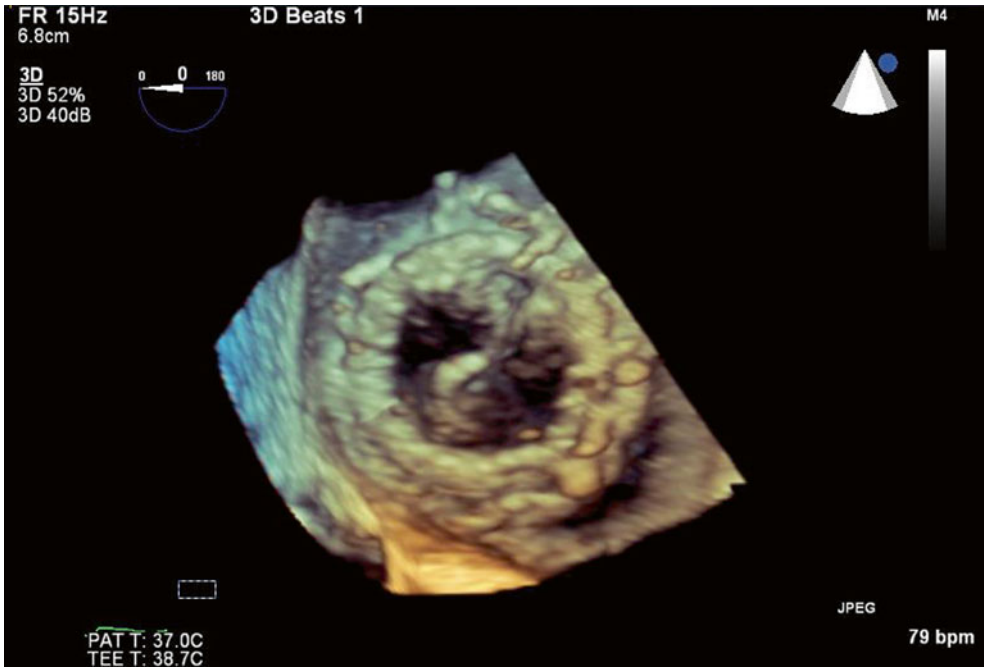

Fig. 11.1 A 3D image of a normally functioning, trileaflet, Biocor bioprosthetic mitral valve replacement viewed from the left atrium. High image resolution enables the leaflets, annulus, and even sutures to be clearly demonstrated. The 3D image is conventionally orientated with the aortic valve at the 12 o'clock position, thereby allowing consistency of image description and better ease of interpretation

11.1 Case 1. Alfieri Stitch

A 70-year-old woman presented with long-standing mitral regurgitation, aortic regurgitation, and paroxysmal atrial fibrillation. She demonstrated increasing left atrial and left ventricular enlargement, which prompted surgical referral. Despite prominent mitral annular calcification, the surgeon was able to successfully repair her mitral valve, using plication of the middle scallop of the posterior leaflet, an Alfieri stitch, and placement of a 35-mm annuloplasty ring. She also underwent replacement of the aortic valve with a #23 Carpentier-Edwards bovine pericardial heterograft, isolation of the pulmonary veins, and ligation of the left atrial appendage (Figs. 11.2, 11.3, 11.4, and 11.5).

Video 11.2 A parasternal long-axis view demonstrates the repaired mitral valve, with the aortic valve replacement in situ (AVI 2992 kb)

Video 11.3 Slight angulation of the probe demonstrates a parasternal long-axis view of the mitral valve at the position of the Alfieri stitch. This appearance may be mistaken for mitral stenosis. The annuloplasty ring in short axis can be best appreciated at the posterior aspect of the annulus (AVI 2244 kb)

Video 11.4 A parasternal short-axis view at the left ventricular base demonstrates the double-orifice mitral valve with the Alfieri stitch joining the middle aspects of both mitral valve leaflets and improving overall leaflet coaptation (AVI 3100 kb)

Video 11.5 The mitral valve is viewed from an apical four-chamber view. The Alfieri stitch can be seen joining the leaflet tips centrally. The annuloplasty ring is appreciated laterally. The posterior leaflet appears small and somewhat restricted, consistent with the known repair and plication of the middle posterior scallop (AVI 2712 kb)

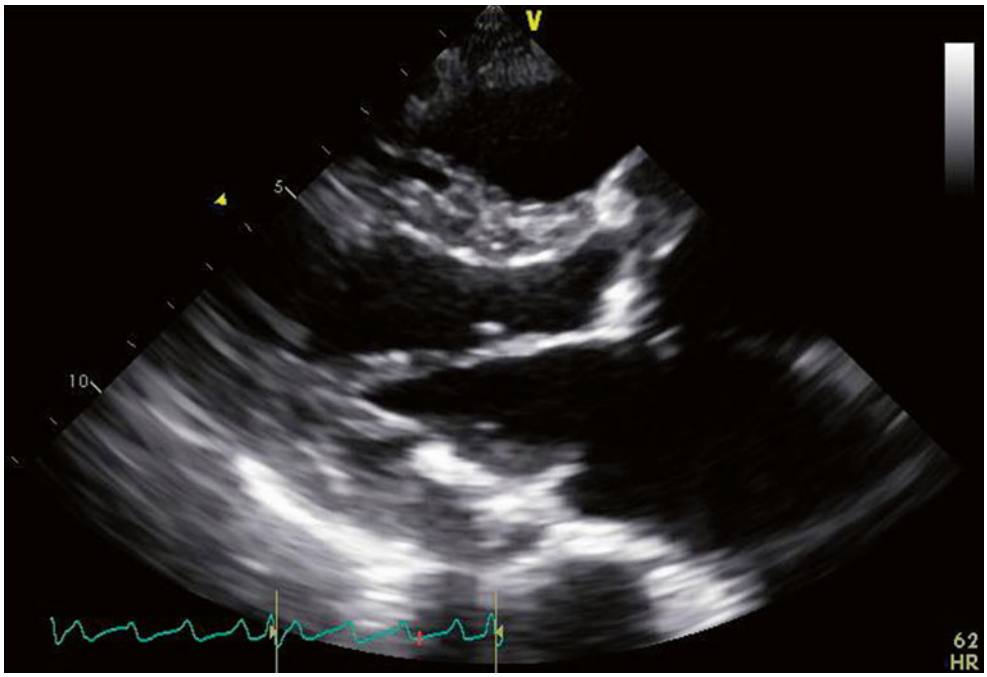

Fig. 11.2 A parasternal long-axis view demonstrates the repaired mitral valve, with the aortic valve replacement in situ

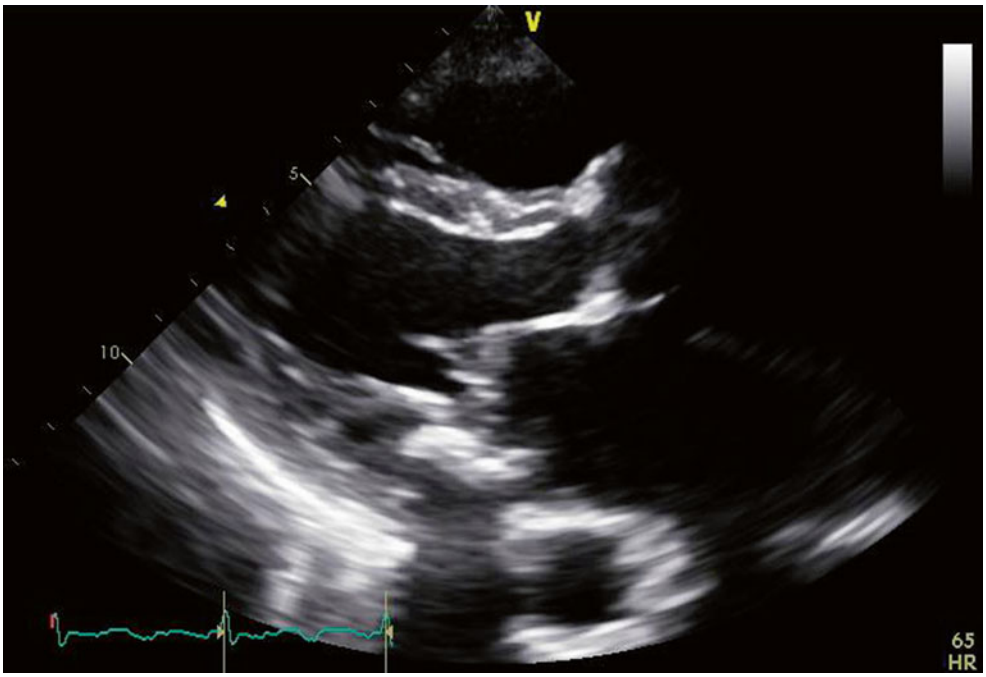

Fig. 11.3 Slight angulation of the probe demonstrates a parasternal long-axis view of the mitral valve at the position of the Alfieri stitch. This appearance may be mistaken for mitral stenosis. The annuloplasty ring in short axis can be best appreciated at the posterior aspect of the annulus

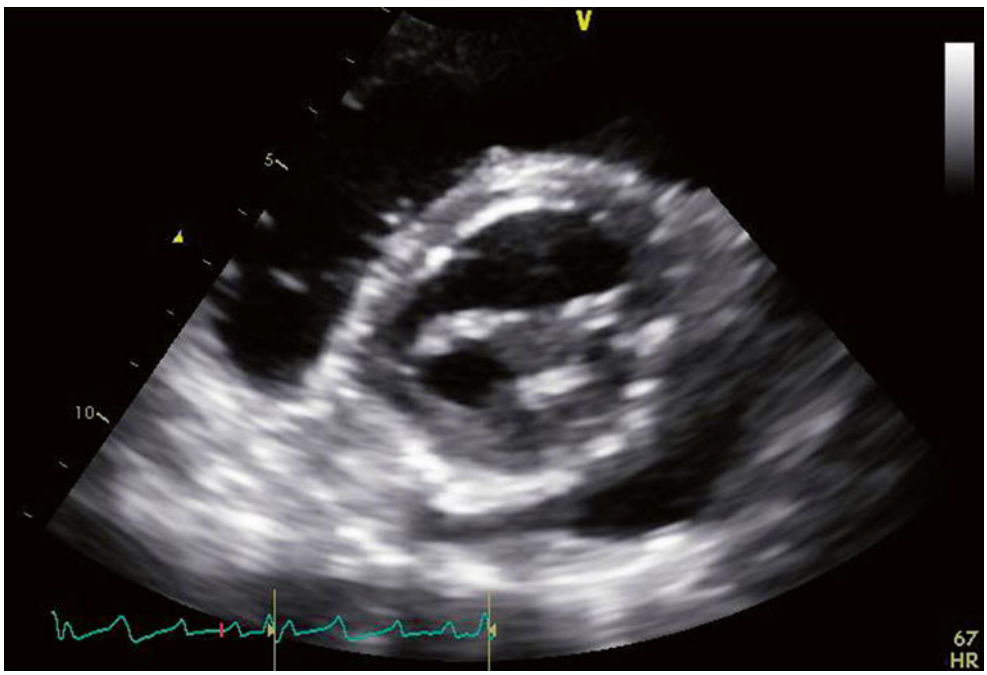

Fig. 11.4 A parasternal short-axis view at the left ventricular base demonstrates the double-orifice mitral valve with the Alfieri stitch joining the middle aspects of both mitral valve leaflets and improving overall leaflet coaptation

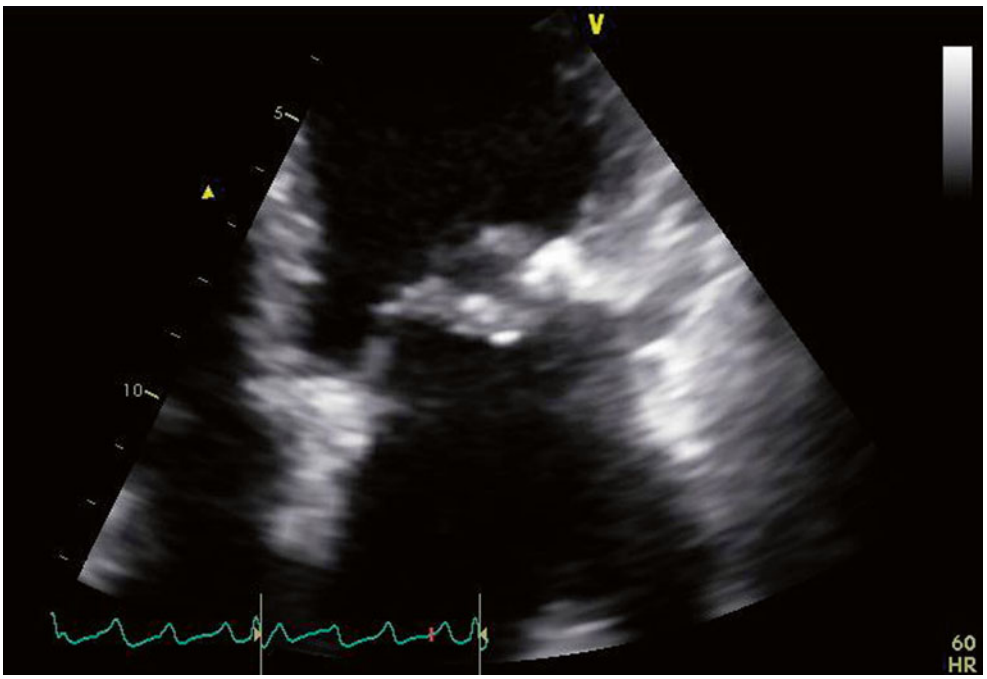

Fig. 11.5 The mitral valve is viewed from an apical four-chamber view. The Alfieri stitch can be seen joining the leaflet tips centrally. The annuloplasty ring is appreciated laterally. The posterior leaflet appears small and somewhat restricted, consistent with the known repair and plication of the middle posterior scallop

11.2 Case 2. Valvuloplasty

A 43-year-old woman in previously excellent health presented with a cerebrovascular accident due to middle cerebral artery occlusion. She was emergently treated with fibrinolysis and achieved full recovery. She subsequently was found to have severe mitral stenosis, despite an absence of previous symptoms. The transvalvular peak gradient was 23 mmHg and the mean gradient was 14 mmHg, with moderate (2–3+) mitral regurgitation. She was anticoagulated and then referred for mitral balloon valvuloplasty, which was performed via a trans-septal puncture. After the procedure, the gradients were reduced to 16 and 9 mmHg, with only mild (1+) residual mitral regurgitation, and the estimated mitral valve area (by pressure half time) was 1.9 cm^2 (Figs. 11.6, 11.7, 11.8, 11.9, 11.10, 11.11, 11.12, and 11.13).

Video 11.6 Transesophageal echocardiogram (TEE) at 0°, demonstrating severe thickening and tethering of both mitral valve leaflets (predominantly involving the leaflet tips). This appearance is typical for rheumatic heart disease (AVI 4855 kb)

Video 11.7 TEE at 0° demonstrating moderate (2–3+) regurgitation at baseline. A septostomy has been performed in preparation for the valvuloplasty, and the catheter can be seen traversing the interatrial septum (AVI 1992 kb)

Video 11.8 A 3D image of the mitral valve viewed from the left atrium. The leaflets are thickened, with commissural fusion and a resultant reduced valve area (AVI 1077 kb)

Video 11.9 Balloon inflation within the mitral valve at the time of valvuloplasty (AVI 6410 kb)

Video 11.10 After valvuloplasty, biplane color Doppler imaging through the mitral valve demonstrates no significant increase in severity of mitral regurgitation from baseline (AVI 1806 kb)

Video 11.11 A 3D image of the mitral valve (viewed from the left atrium) after valvuloplasty shows that leaflet mobility has improved, with a reduction in commissural fusion and an increased valve area (AVI 1272 kb)

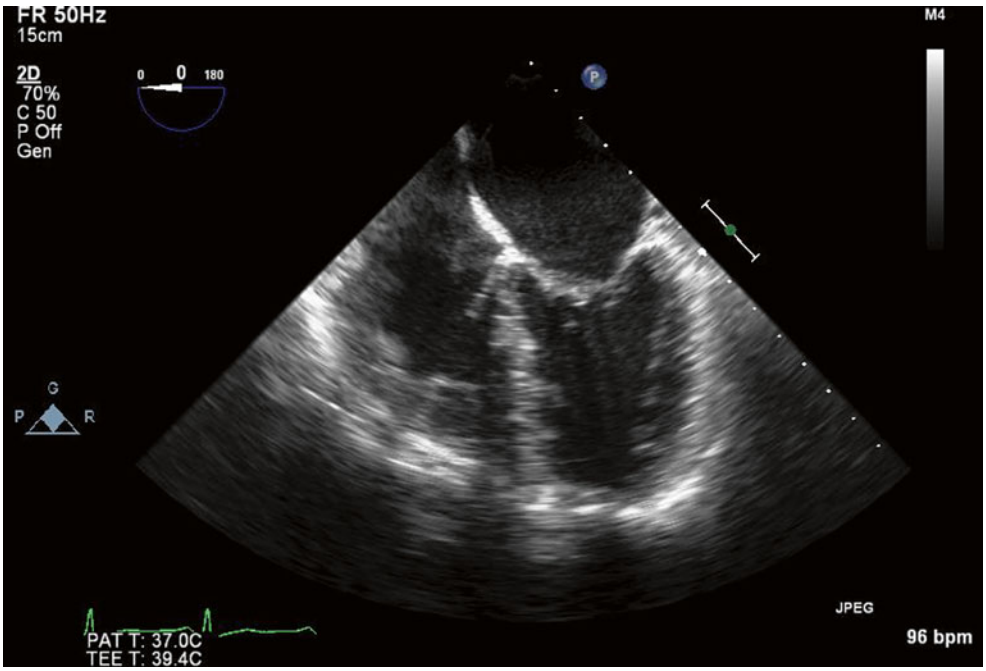

Fig. 11.6 Transesophageal echocardiogram (TEE) at 0°, demonstrating severe thickening and tethering of both mitral valve leaflets (predominantly involving the leaflet tips). This appearance is typical for rheumatic heart disease

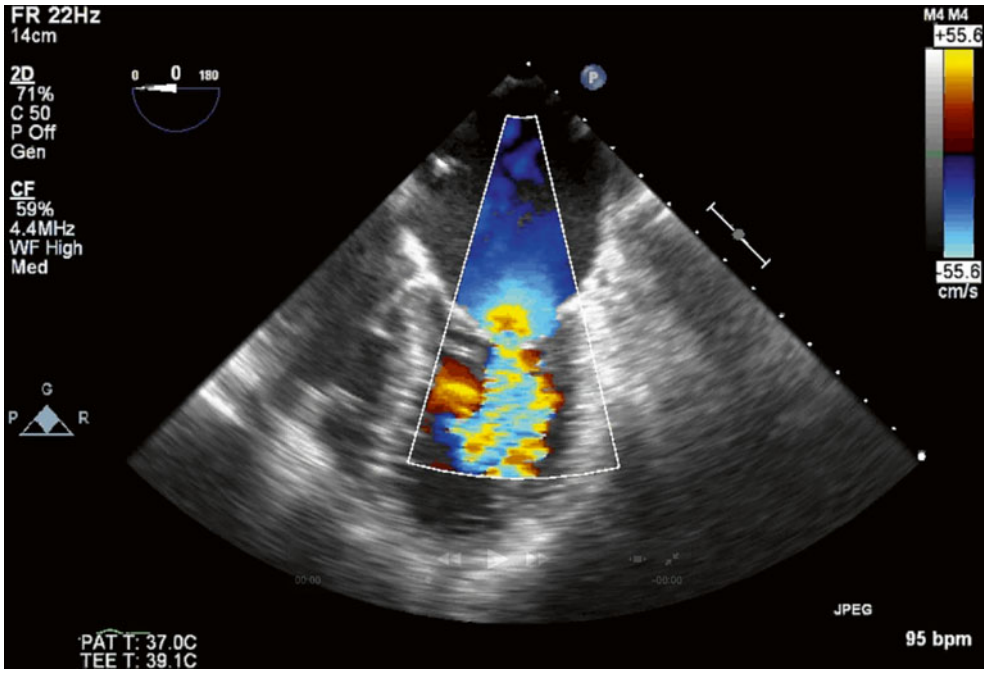

Fig. 11.7 TEE at 0° demonstrating moderate (2–3+) regurgitation at baseline. A septostomy has been performed in preparation for the valvuloplasty, and the catheter can be seen traversing the interatrial septum

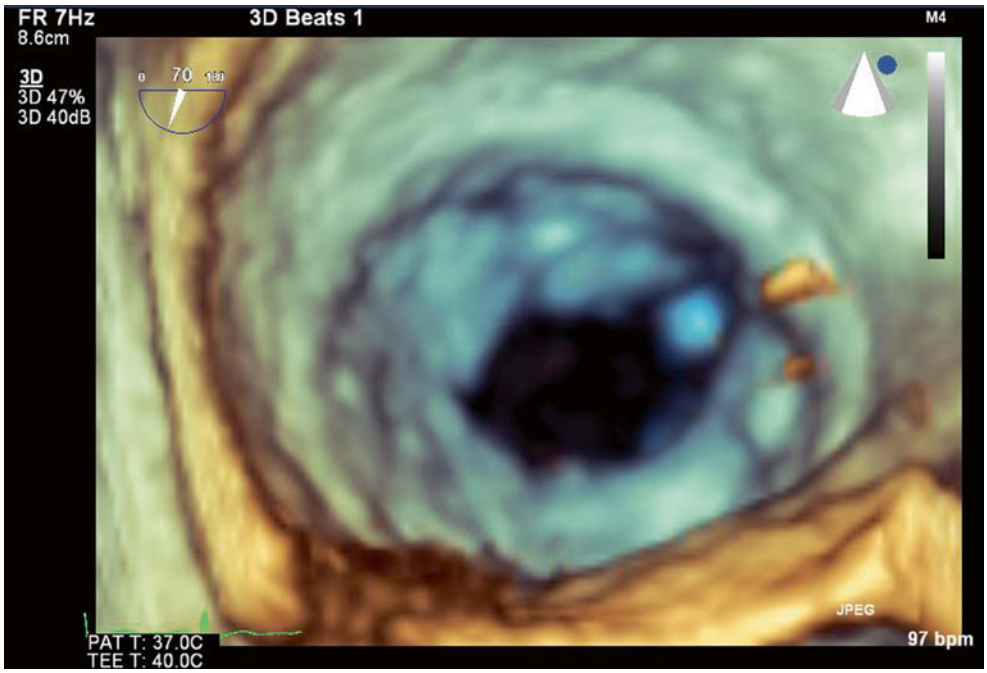

Fig. 11.8 3D image of the mitral valve viewed from the left atrium. The leaflets are thickened, with commissural fusion and a resultant reduced valve area

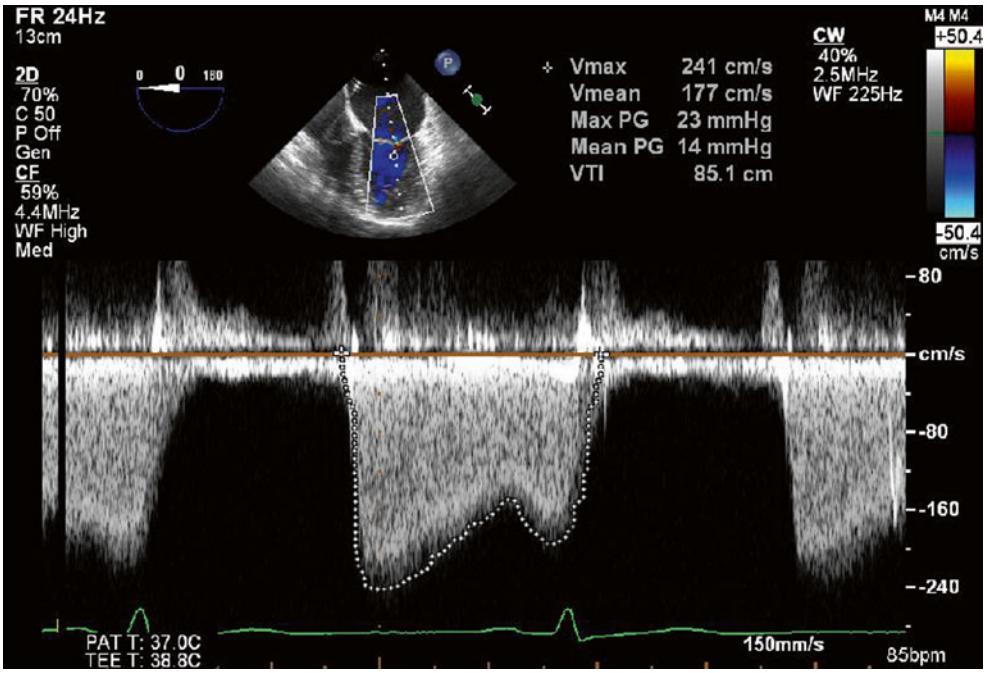

Fig. 11.9 Continuous wave Doppler through the mitral valve demonstrates severe stenosis with a peak gradient of 23 mmHg and a mean gradient of 14 mmHg

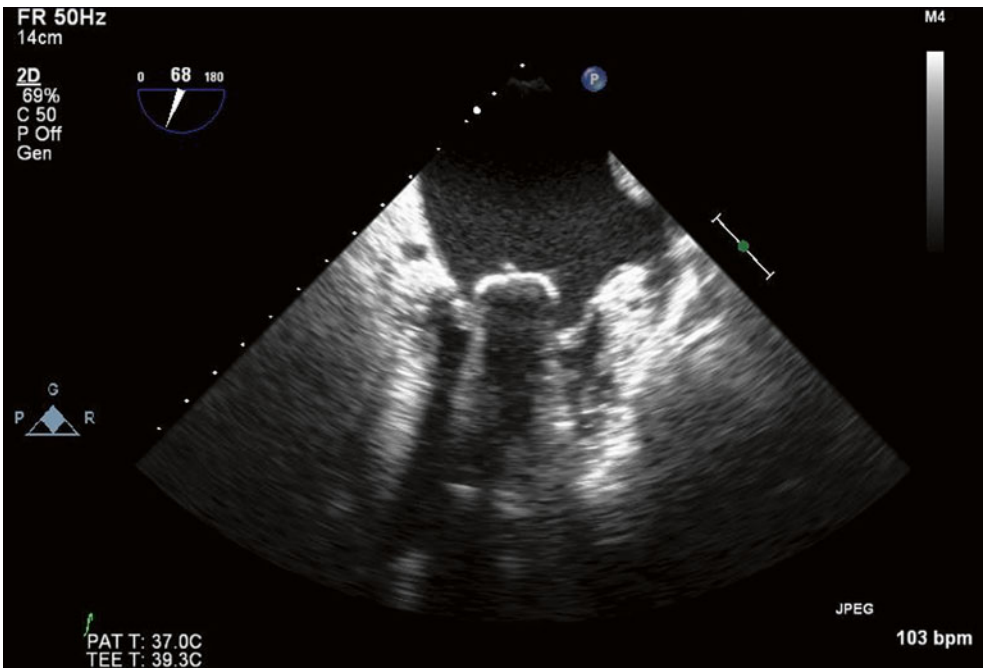

Fig. 11.10 Balloon inflation within the mitral valve at the time of valvuloplasty

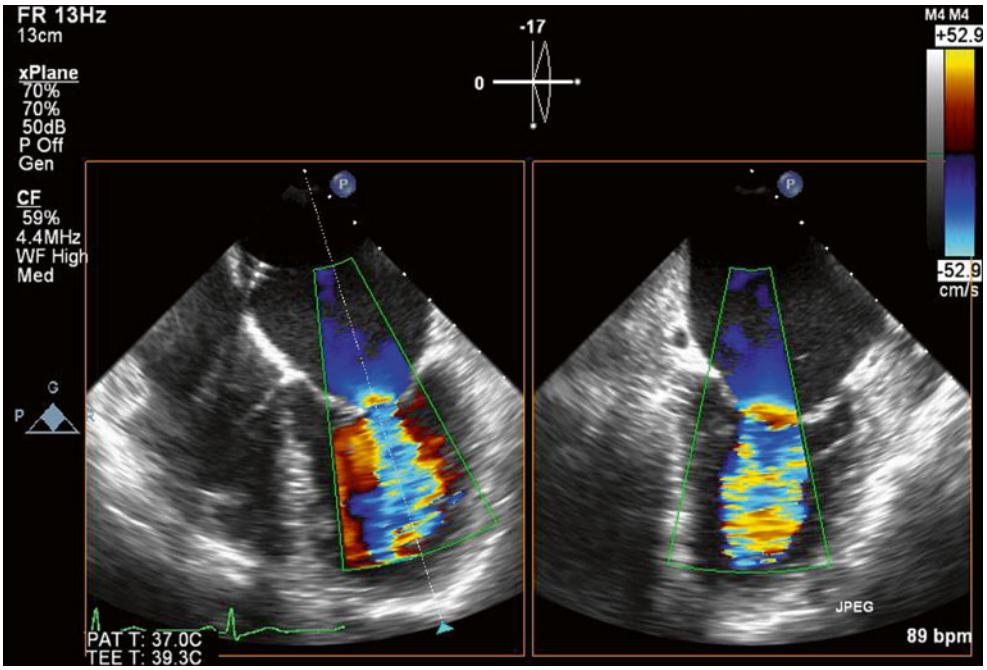

Fig. 11.11 After valvuloplasty, biplane color Doppler imaging through the mitral valve demonstrates no significant increase in severity of mitral regurgitation from baseline

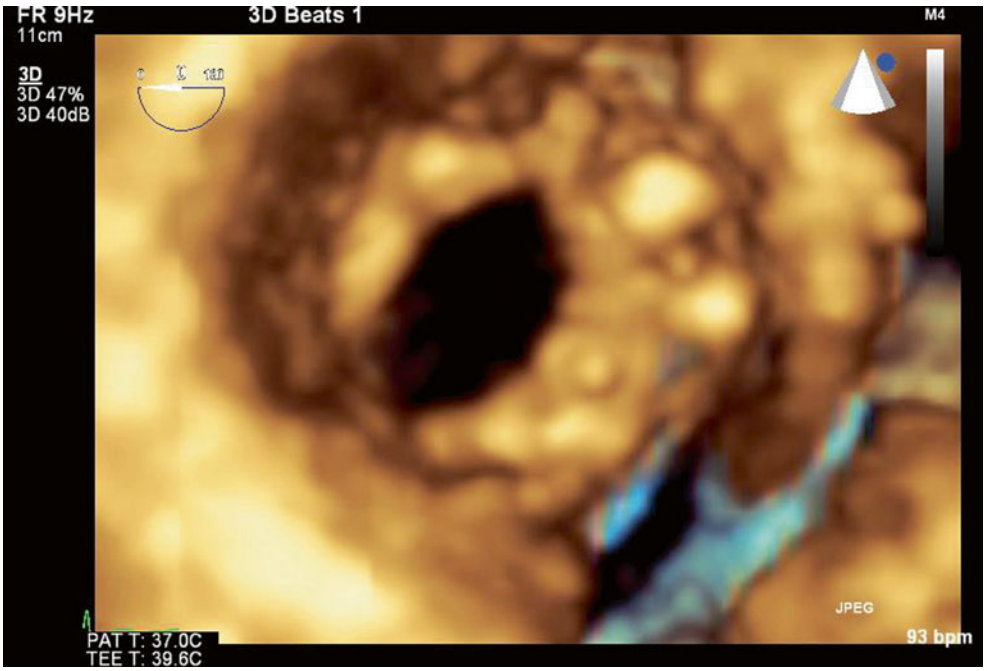

Fig. 11.12 A 3D image of the mitral valve (viewed from the left atrium) after valvuloplasty shows that leaflet mobility has improved, with a reduction in commissural fusion and an increased valve area

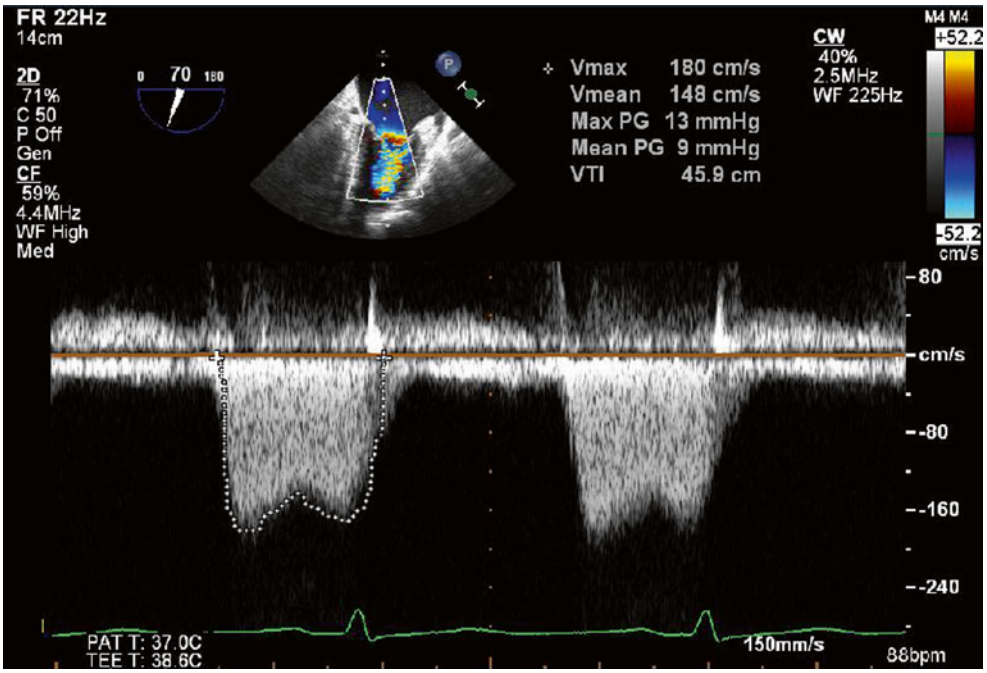

Fig. 11.13 Continuous wave Doppler through the mitral valve after valvuloplasty demonstrates an improvement in transmitral gradients to a peak of 13 mmHg and a mean of 9 mmHg

11.3 Case 3. Paravalvular Leak 1

A 62-year-old woman with end-stage renal failure on hemodialysis presented with a severe paravalvular mitral valve leak, severe tricuspid regurgitation, and moderate aortic stenosis on a background history of previous bioprosthetic mitral valve replacement and coronary artery bypass graft surgery 3 years earlier. She underwent a mitral valve replacement with an On-X mechanical valve (#33), a tricuspid valve repair with a Carpentier ring (#30), an aortic valve replacement with a Trifecta bioprosthesis (#23), and coronary artery bypass graft surgery.

Preoperative echocardiography demonstrated a paravalvular leak originating at the anterolateral aspect of the mitral annulus. The eccentric, regurgitant jet hugged the wall of the left atrium and was difficult to quantitate, but visually it appeared severe. Transvalvular peak and mean gradients of 17 and 9 mmHg were noted (Figs. 11.14, 11.15, and 11.16).

Video 11.12 TEE at 50° demonstrates an eccentric paravalvular leak originating at the anterolateral aspect of the mitral annulus (AVI 1485 kb)

Video 11.13 With 3D reconstruction of the mitral valve, orientated with the aortic valve at the top of the image, the small paravalvular defect can be seen adjacent to the valve annulus at the 6 o'clock position (AVI 845 kb)

Video 11.14 Color 3D imaging clearly demonstrates the small paravalvular leak (AVI 953 kb)

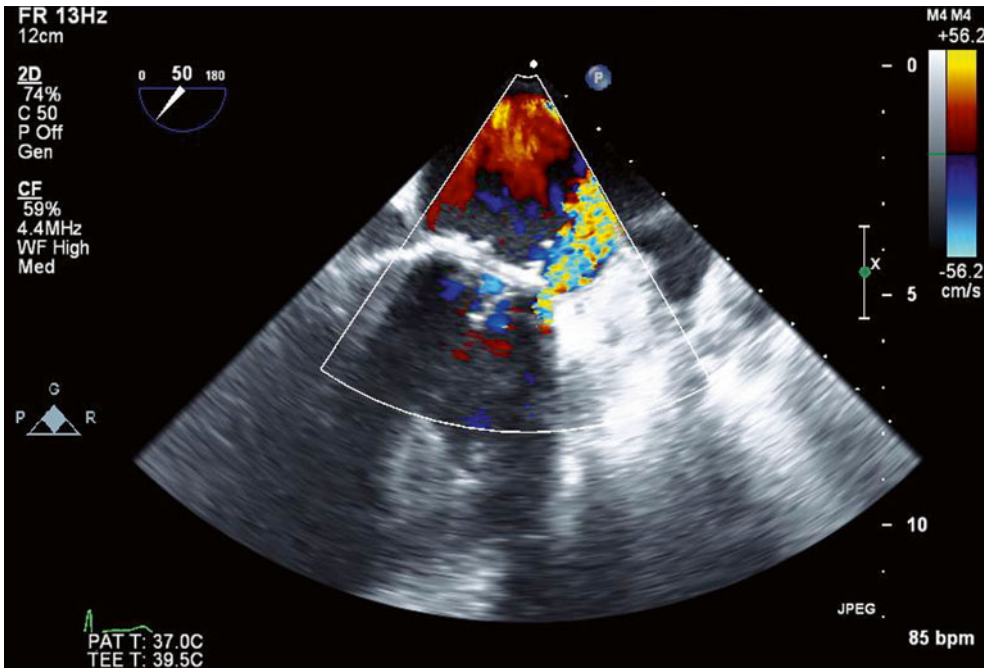

Fig. 11.14 TEE at 50° demonstrates an eccentric paravalvular leak originating at the anterolateral aspect of the mitral annulus

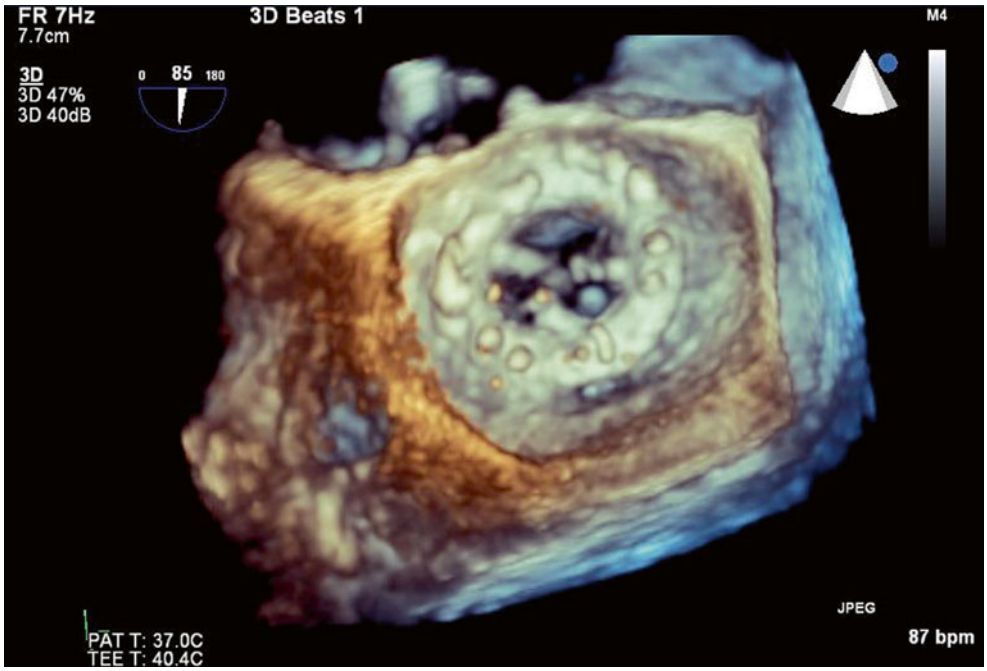

Fig. 11.15 With 3D reconstruction of the mitral valve, orientated with the aortic valve at the top of the image, the small paravalvular defect can be seen adjacent to the valve annulus at the 6 o'clock position

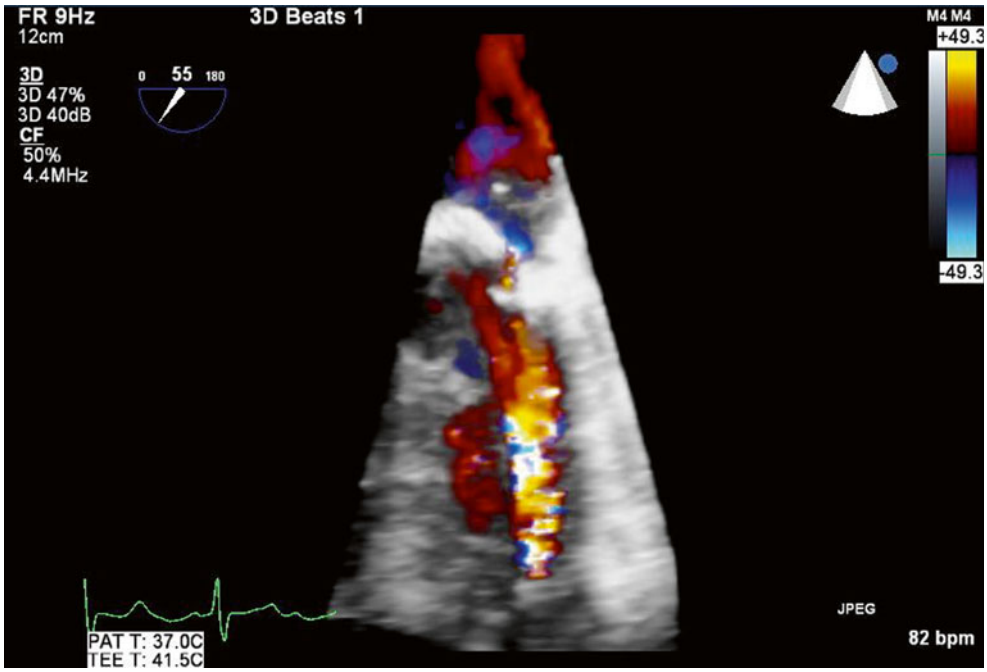

Fig. 11.16 3D color Doppler imaging clearly demonstrates the small paravalvular leak

11.4 Case 4. Paravalvular Leak 2

A 51-year-old woman with a past history of mitral valve replacements 20 and 27 years previously now presents with hemolytic anemia, atrial fibrillation, and a small (5 mm) mitral paravalvular leak with severe tricuspid regurgitation. She has symptoms of right heart failure with evidence of fluid overload. She has known biventricular dysfunction, with implantation of an implantable cardiac defibrillator.

Echocardiography demonstrated biventricular enlargement. The St. Jude mechanical prosthetic mitral valve replacement was associated with a moderate (2–3+), posterolaterally directed paravalvular leak, which originated adjacent to the lateral aspect of the valve near the left atrial appendage ostium, although the valve itself remained well seated. There was severe (4+) tricuspid regurgitation related to annular dilatation.

She successfully underwent her third cardiac surgery involving mitral valve replacement with an On-X mechanical valve (#33) and a tricuspid valve repair with a Carpentier classic annuloplasty ring (#30) (Figs. 11.17, 11.18, 11.19, and 11.20).

Video 11.15 TEE at 60° demonstrating the mechanical mitral valve with normally functioning leaflets. A small paravalvular region of defect can be seen adjacent to the lateral aspect of the valve (AVI 8981 kb)

Video 11.16 The same 60° TEE view demonstrates a small jet of flow through the paravalvular defect on color Doppler imaging (AVI 1539 kb)

Video 11.17 Rotating the TEE probe to 90° demonstrates the paravalvular leak adjacent to the lateral aspect of the valve, perpendicular to the orifice of the left atrial appendage (AVI 1689 kb)

Video 11.18 3D imaging of the mechanical mitral valve demonstrates a normally functioning, well-seated bileaflet prosthesis (AVI 1277 kb)

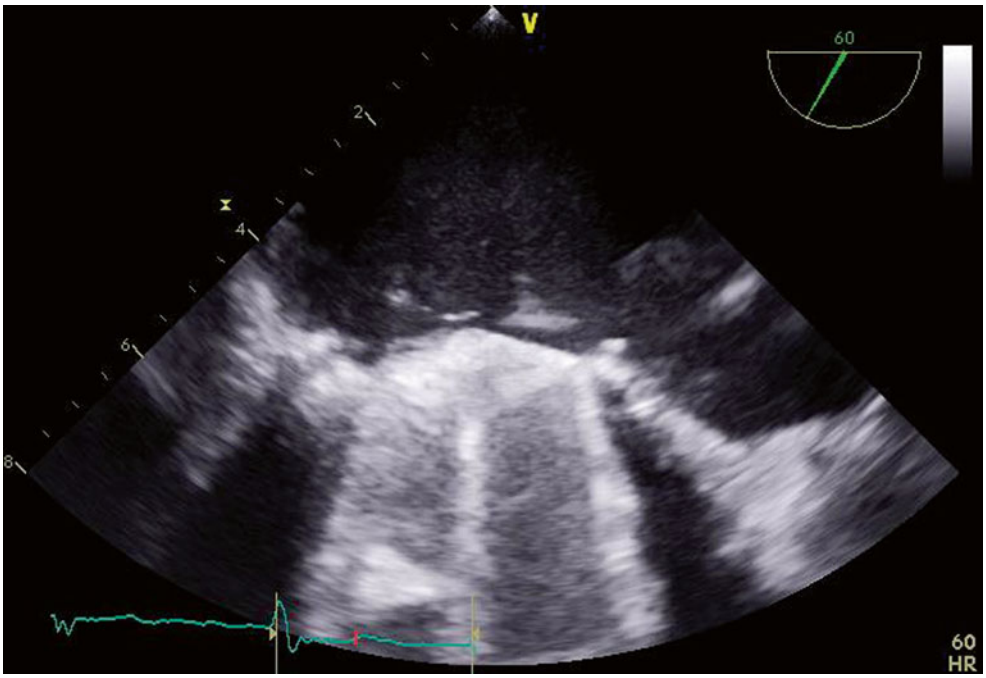

Fig. 11.17 TEE at 60° demonstrating the mechanical mitral valve with normally functioning leaflets. A small paravalvular region of defect can be seen adjacent to the lateral aspect of the valve

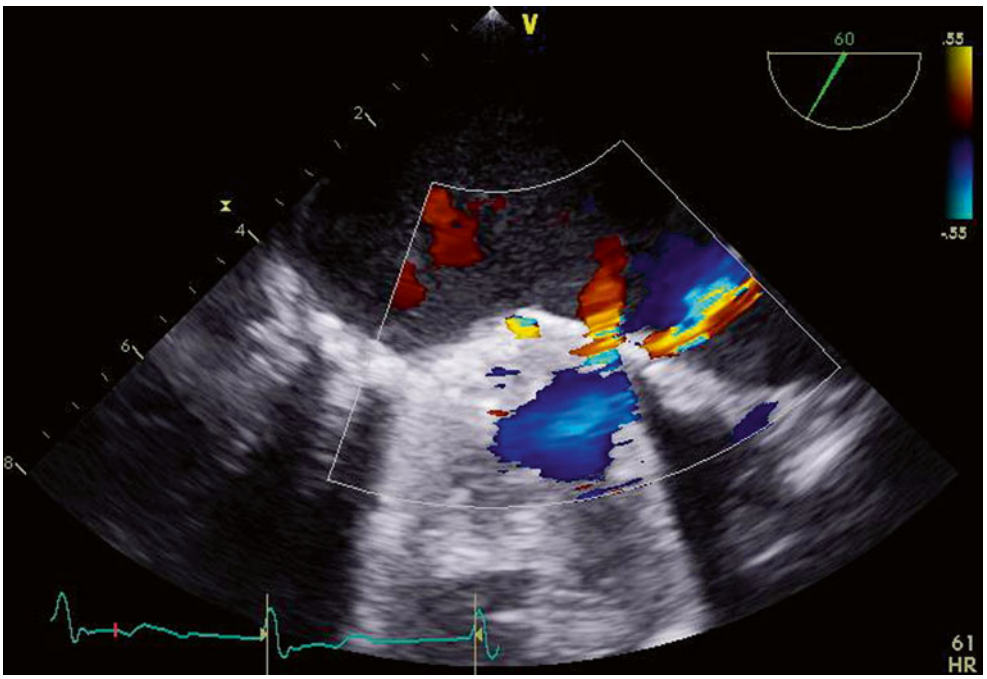

Fig. 11.18 The same 60° transesophageal view demonstrates a small jet of flow through the paravalvular defect on color Doppler imaging

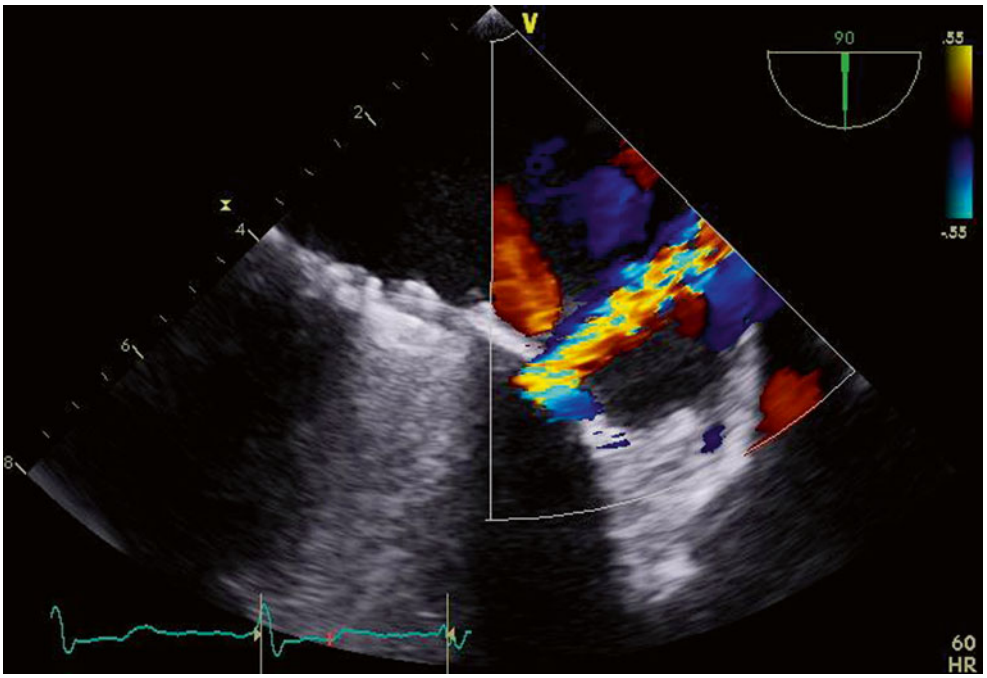

Fig. 11.19 Rotating the transesophageal probe to 90° demonstrates the paravalvular leak adjacent to the lateral aspect of the valve, perpendicular to the orifice of the left atrial appendage

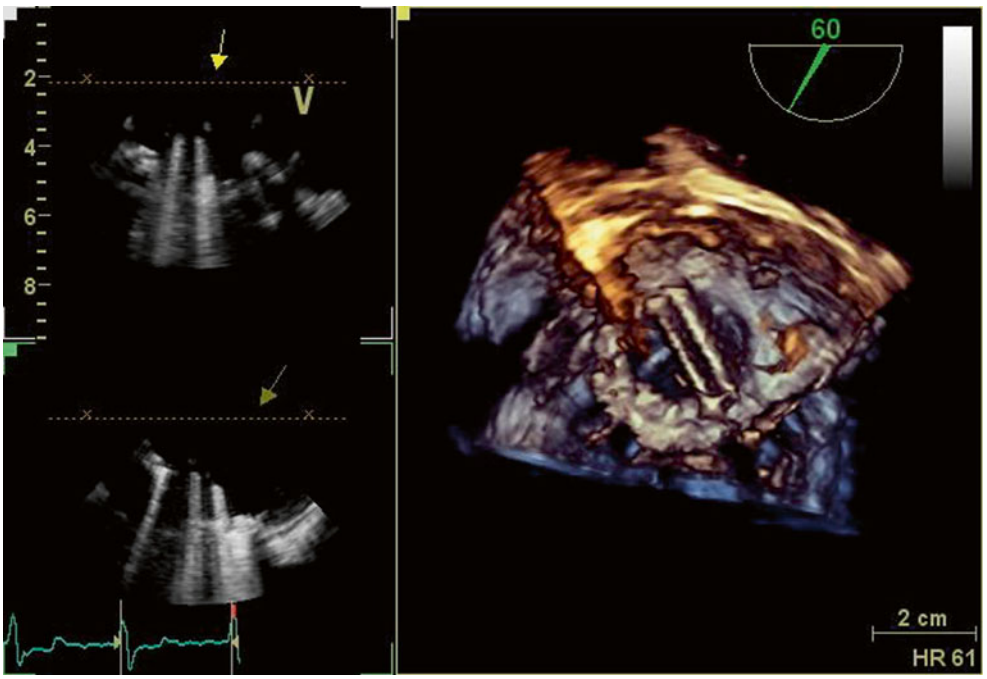

Fig. 11.20 3D imaging (*right-hand panel*) of the mechanical mitral valve demonstrates a normally functioning, well-seated bileaflet prosthesis

11.5 Case 5. Paravalvular Leaks 3

A 67-year-old woman presented with mild exertional dyspnea and mild hemolytic anemia. Her background history included myxomatous mitral valve disease, for which she underwent mitral valve replacement over 10 years ago, followed by replacement with a porcine valve and tricuspid repair 3 years ago.

Transthoracic and transesophageal echocardiograms were remarkable for a moderate (2+), anterolateral mitral paravalvular leak, although the mitral valve prosthesis appeared otherwise well-seated. The vena contracta measured 0.1 cm^2. Otherwise, there was only trivial valvular regurgitation, with no restriction of leaflet excursion. The peak and mean gradients were 22 and 6 mmHg. The tricuspid valve repair appeared intact, with only trivial regurgitation and a mean gradient of 4 mmHg (Figs. 11.21, 11.22, 11.23, and 11.24).

Given her lack of symptoms and only mild anemia, she will have ongoing follow-up with serial echocardiography every 6–12 months, or sooner if her symptoms worsen.

Video 11.19 Transesophageal long-axis view demonstrating a normally functioning bioprosthetic mitral valve replacement (AVI 4234 kb)

Video 11.20 Transesophageal long-axis view with a moderate (2+) paravalvular leak anteriorly on color Doppler imaging (AVI 2679 kb)

Video 11.21 3D left atrial view of the mitral valve, atypically orientated with the aortic valve at 3 o'clock and the anterior paravalvular defect at the 9 o'clock position (AVI 745 kb)

Video 11.22 3D left ventricular view of the mitral valve, with the anterior paravalvular defect now visible at the 3 o'clock position (AVI 755 kb)

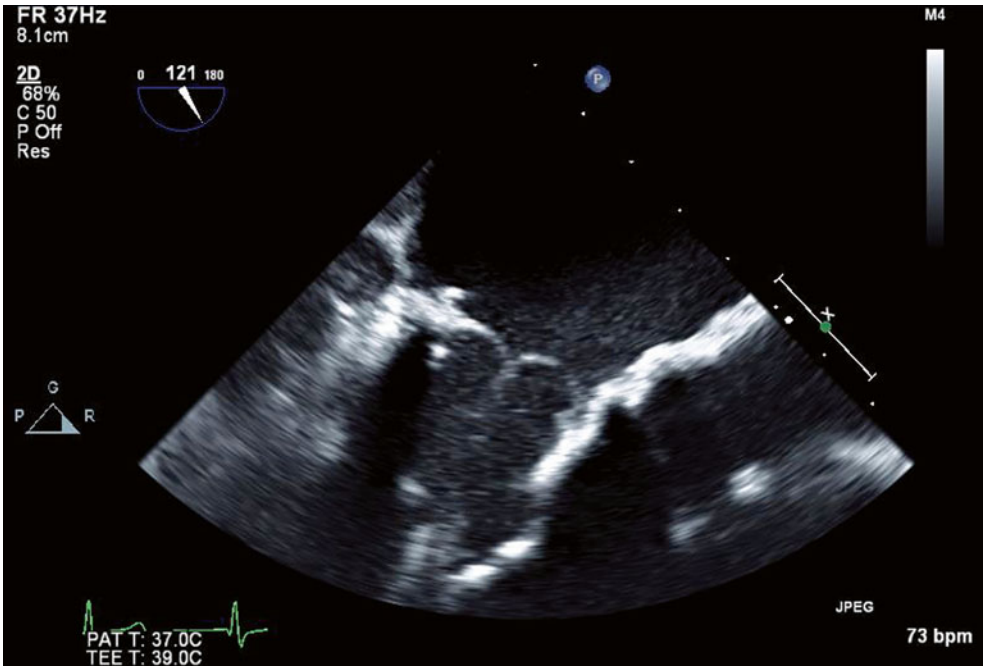

Fig. 11.21 TEE long-axis view demonstrating a normally functioning bioprosthetic mitral valve replacement

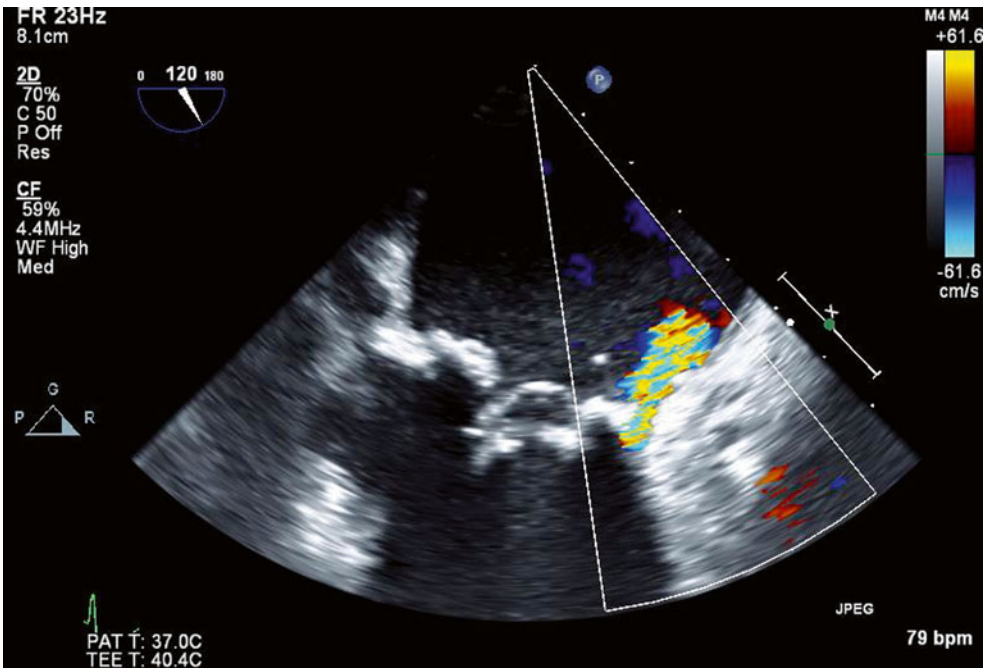

Fig. 11.22 TEE long-axis view with a moderate (2+) paravalvular leak anteriorly on color Doppler imaging

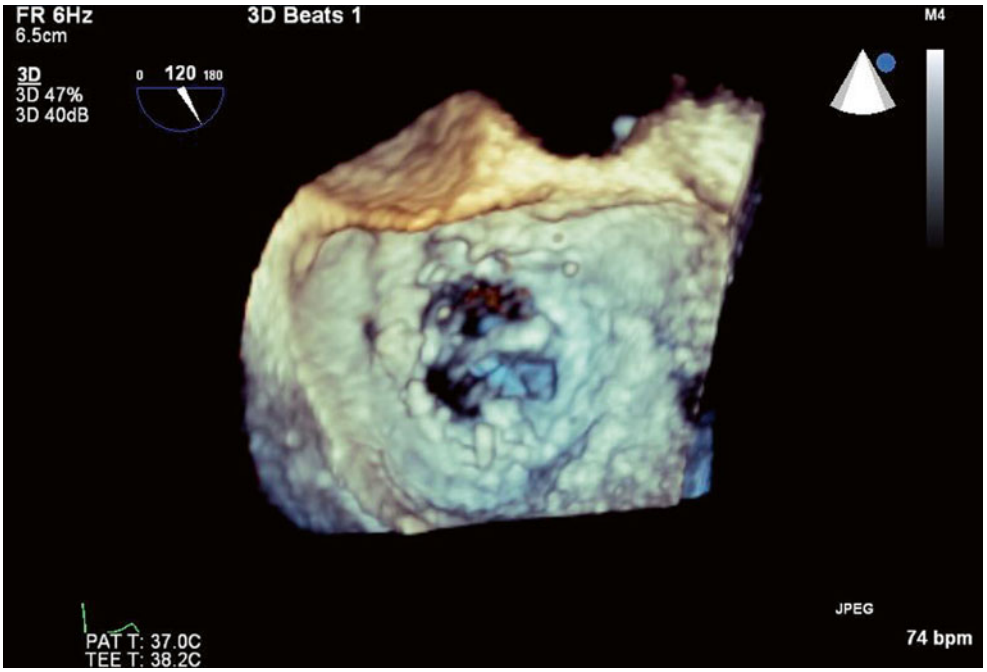

Fig. 11.23 3D left atrial view of the mitral valve, atypically orientated with the aortic valve at 3 o'clock and the anterior paravalvular defect at the 9 o'clock position

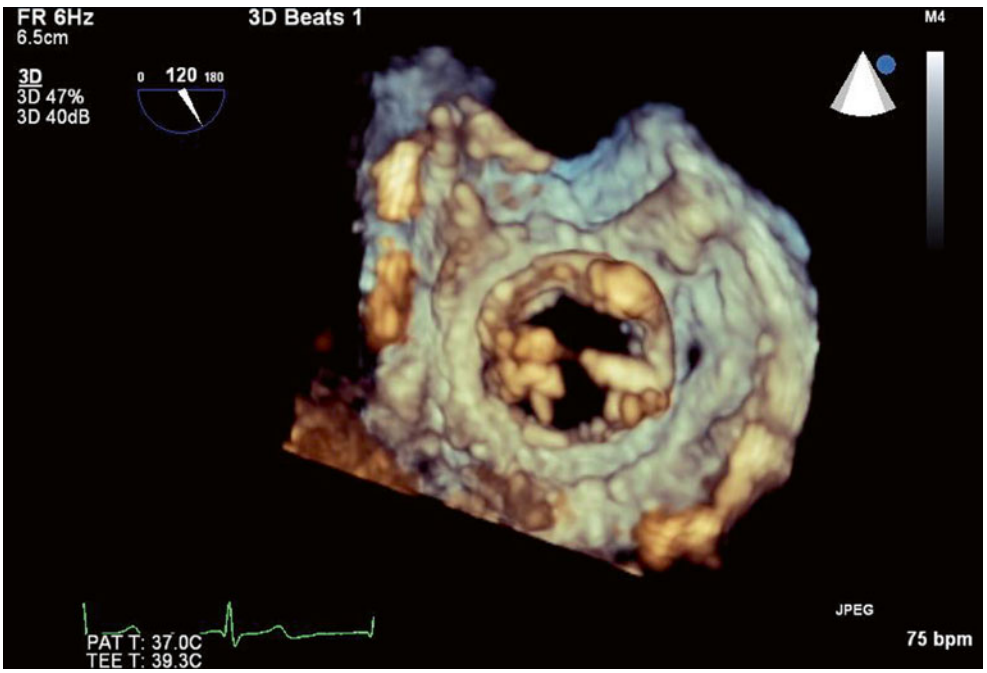

Fig. 11.24 3D left ventricular view of the mitral valve, with the anterior paravalvular defect now visible at the 3 o'clock position

11.6 Case 6. Bioprosthetic Mitral Valve Replacement and Pseudoaneurysm

A 77-year-old woman was referred with a history of coronary artery bypass graft surgery and bioprosthetic aortic (#21) and mitral (#25) valve replacements for aortic stenosis and mitral regurgitation 2 months earlier. The surgery had been complicated by severe mitral annular calcification and bleeding from the AV groove and posterior ventricle, which required a pericardial patch. She now reported worsening symptoms of heart failure, and echocardiography demonstrated partial dehiscence of the mitral valve with a resultant severe, posterior paravalvular leak (measuring 1.0 cm in maximal diameter), which was in direct communication with a large (5.0×4.1 cm) pseudoaneurysm adjacent to the left atrium, which obstructed pulmonary venous drainage (Figs. 11.25, 11.26, 11.27, and 11.28). The aortic valve replacement was well seated, with only trivial regurgitation. Reoperation was performed involving removal of the old prosthesis, unroofing and repair of the pseudoaneurysm, and replacement of the mitral valve with a Biocor #29 prosthesis.

Video 11.23 TEE imaging of the bioprosthetic mitral valve replacement at 38°, demonstrating the large pseudoaneurysm adjacent to the valve annulus and left atrium laterally (AVI 4606 kb)

Video 11.24 The addition of color Doppler imaging demonstrates regurgitant flow directly from the left ventricle into the pseudoaneurysm via a communication located just below the level of the valve annulus laterally (AVI 2413 kb)

Video 11.25 Transesophageal biplane view of the bioprosthetic mitral valve replacement at 0 and 90°, demonstrating the large lateral pseudoaneurysm, which expands during systole, when there is retrograde flow into the cavity (AVI 3898 kb)

Video 11.26 3D reconstruction of the mitral valve viewed from the left atrium. The large pseudoaneurysm can be seen adjacent to the lateral aspect of the valve and left atrium (AVI 1886 kb)

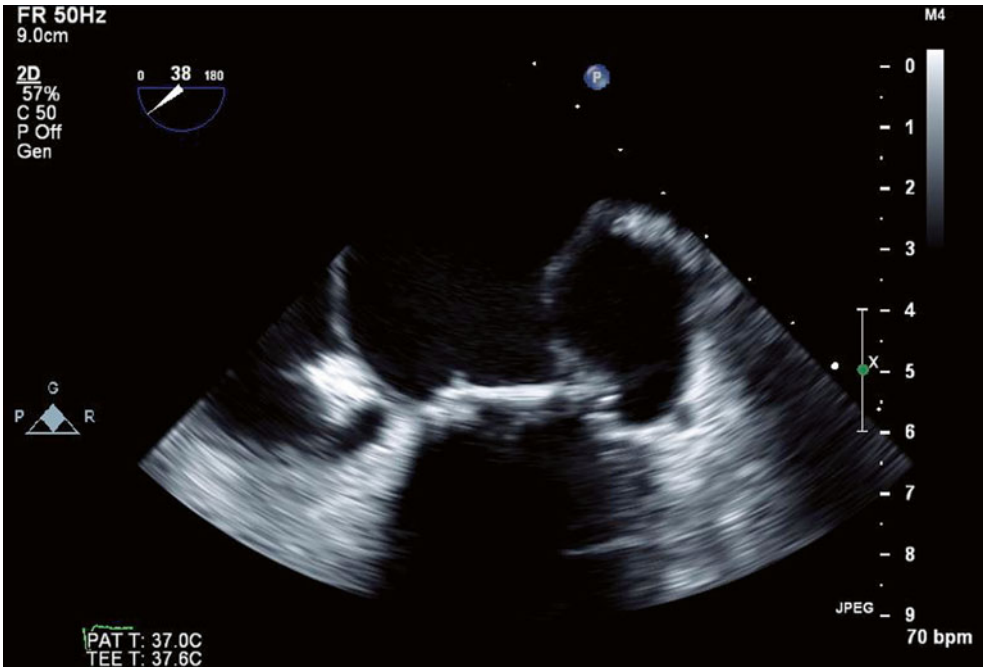

Fig. 11.25 TEE imaging of the bioprosthetic mitral valve replacement at 38°, demonstrating the large pseudoaneurysm adjacent to the valve annulus and left atrium laterally

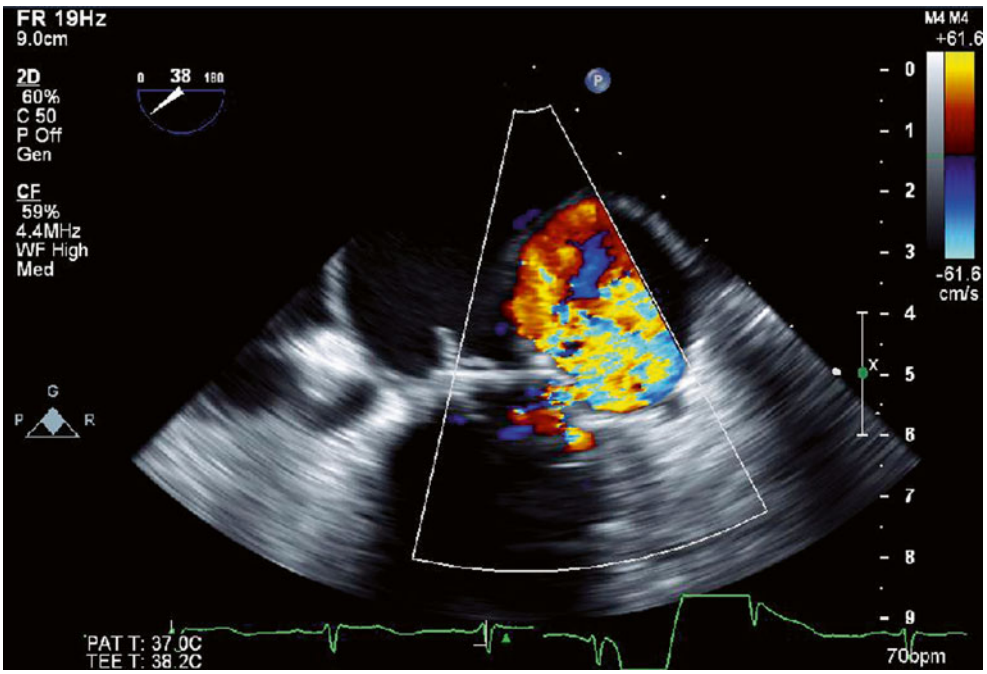

Fig. 11.26 The addition of color Doppler imaging demonstrates regurgitant flow directly from the left ventricle into the pseudoaneurysm via a communication located just below the level of the valve annulus laterally

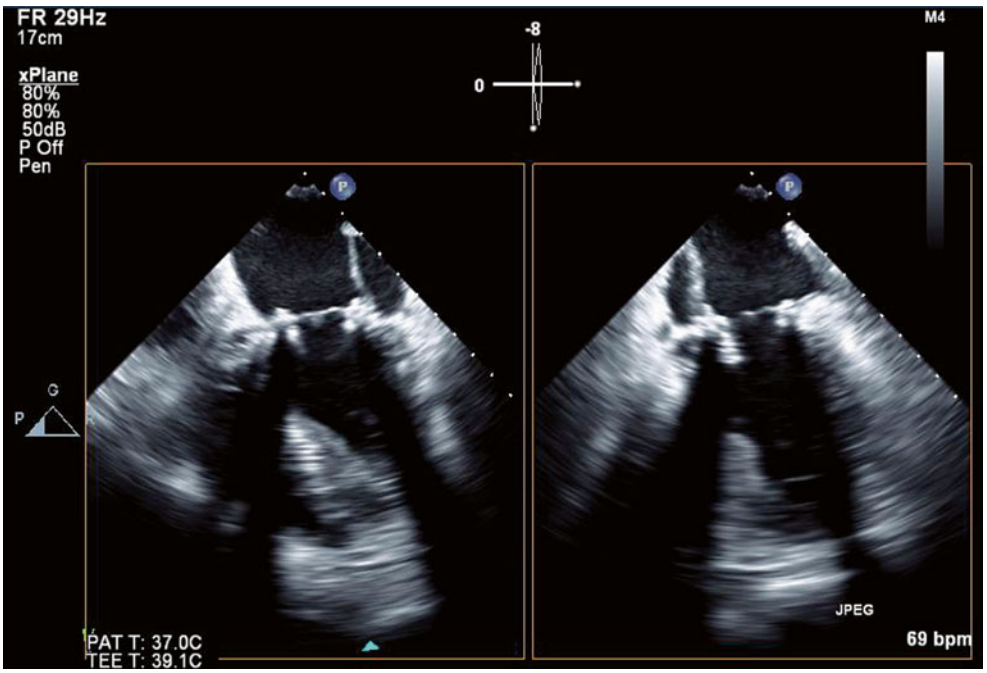

Fig. 11.27 Transesophageal biplane view of the bioprosthetic mitral valve replacement at 0 and 90°, demonstrating the large lateral pseudoaneurysm, which expands during systole, when there is retrograde flow into the cavity

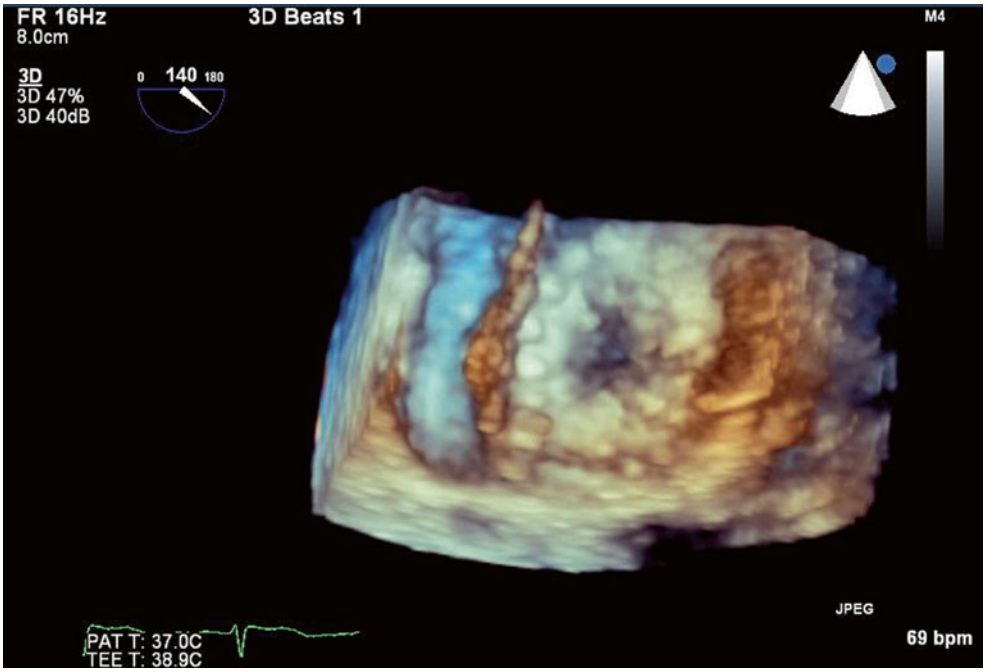

Fig. 11.28 3D reconstruction of the mitral valve viewed from the left atrium. The large pseudoaneurysm can be seen adjacent to the lateral aspect of the valve and left atrium

11.7 Case 7. Mechanical Valve Replacement and Pseudoaneurysm

A 33-year-old man presents with increasing dyspnea and fatigue. His past history was remarkable for bileaflet mechanical mitral valve replacement 5 years earlier, as a result of mitral valve infection endocarditis secondary to intravenous drug use. He has abstained from drug use since this time and remained compliant with oral anticoagulation, but he has not had an echocardiogram for several years.

Echocardiography was performed and demonstrated a mechanical mitral valve replacement with moderate (2+) valvular regurgitation, a moderate (2+) paravalvular jet with flow directed into the left atrial appendage, and a further small paravalvular leak communicating with a small lateral pseudoaneurysm located between the valve annulus and the left atrial appendage (Figs. 11.29, 11.30, and 11.31). Given his lack of constitutional symptoms and negative blood cultures, it was suspected that the pseudoaneurysm was related to an old abscess cavity rather than active infection.

He was taken to the operating room, where the echocardiographic findings were confirmed. The mitral valve prosthesis was left alone, as it appeared normal and was well seated, with preserved function. The pseudoaneurysm was resected, and a patch repair of remaining paravalvular defects was performed. There was no evidence of infective endocarditis or abscess formation visually or on microbiology of the resected tissue.

Video 11.27 TEE imaging of the bileaflet mechanical mitral valve prosthesis at 58°. The valve appears well seated, with normal leaflet opening. A large left atrial appendage can be seen laterally to the right of the image. Between the appendage and the valve is a small cavity demonstrating expansion during systole. This dynamic appearance is suggestive of a pseudoaneurysm (AVI 4572 kb)

Video 11.28 Color Doppler imaging, in the same 58° TEE plane, demonstrates three separate jets of systole flow. There is a moderate (2+) valvular regurgitant jet, a moderate (2+) paravalvular jet originating laterally with flow directed into the left atrial appendage, and a small amount of systolic flow going directly from the left ventricle into the pseudoaneurysm (AVI 1335 kb)

Video 11.29 A 3D reconstruction of the mitral valve prosthesis from the left atrial aspect. The valve appears well seated, with normal motion of both leaflets. The large left atrial appendage can be seen adjacent to the valve laterally to the left of the image. Between the appendage and the valve ring is a small slit-like annular defect (9 o'clock position), which represents the cause of the paravalvular leak (AVI 927 kb)

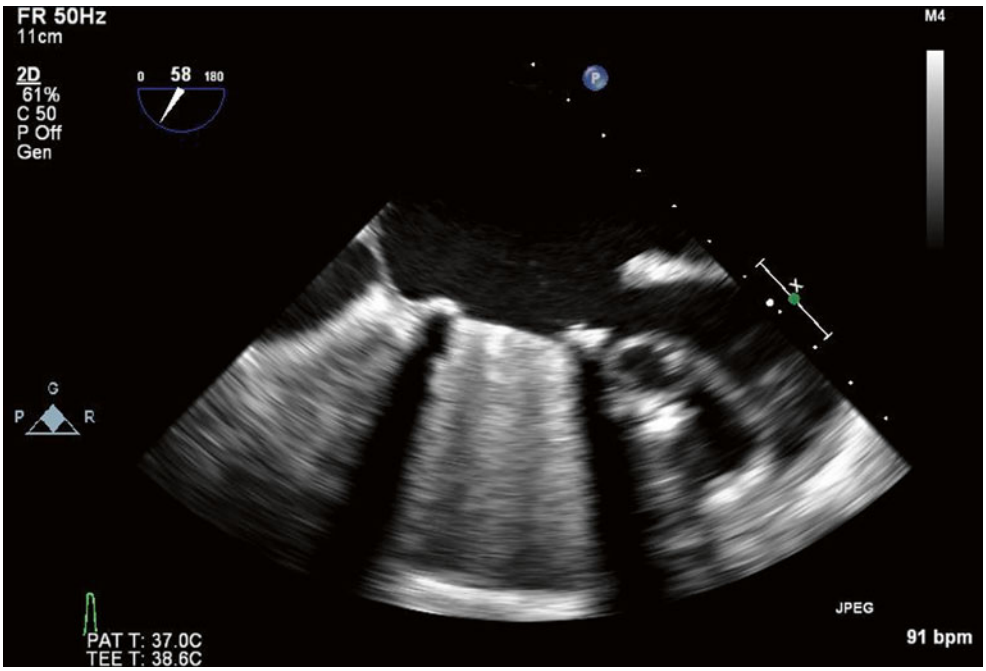

Fig. 11.29 TEE imaging of the bileaflet mechanical mitral valve prosthesis at 58°. The valve appears well seated, with normal leaflet opening. A large left atrial appendage can be seen laterally to the right of the image. Between the appendage and the valve is a small cavity demonstrating expansion during systole. This dynamic appearance is suggestive of a pseudoaneurysm

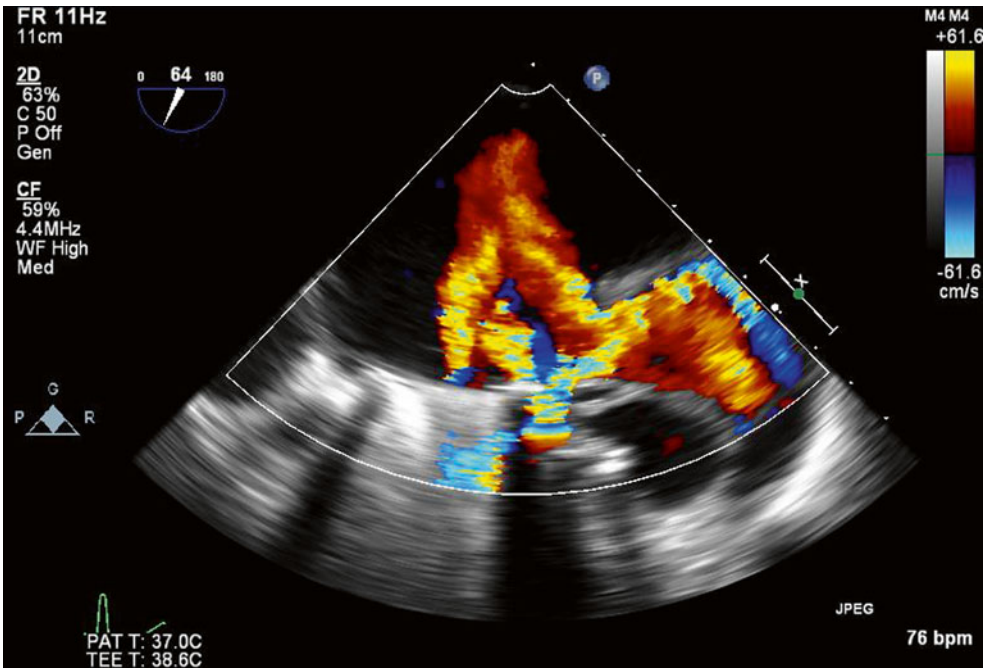

Fig. 11.30 Color Doppler imaging, in the same 58° TEE plane, demonstrates three separate jets of systole flow. There is a moderate (2+) valvular regurgitant jet, a moderate (2+) paravalvular jet originating laterally with flow directed into the left atrial appendage, and a small amount of systolic flow going directly from the left ventricle into the pseudoaneurysm

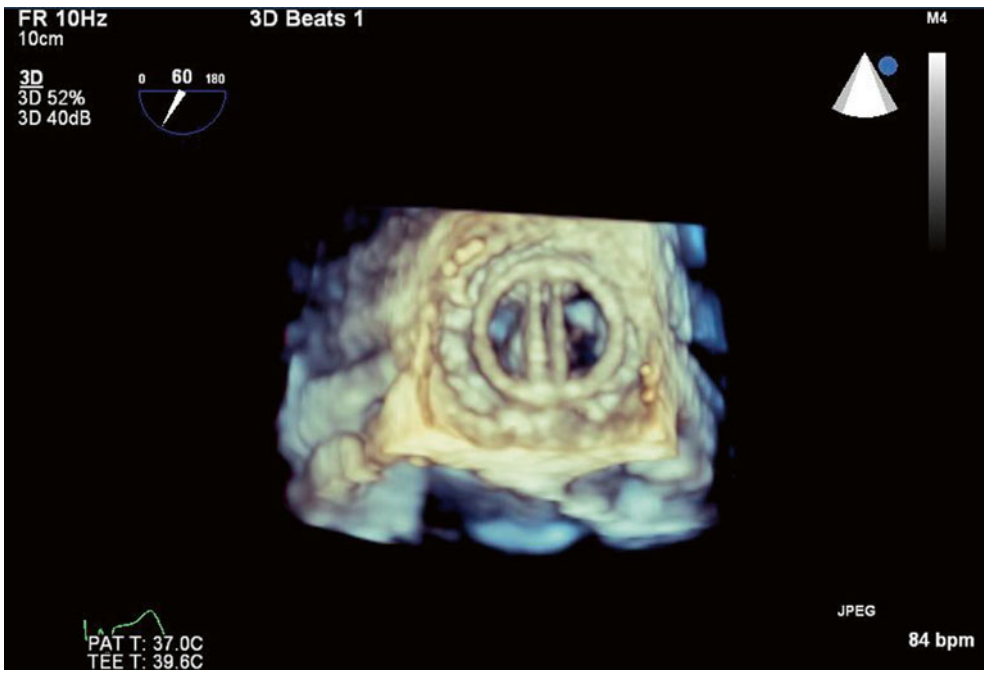

Fig. 11.31 A 3D reconstruction of the mitral valve prosthesis from the left atrial aspect. The valve appears well seated, with normal motion of both leaflets. The large left atrial appendage can be seen adjacent to the valve laterally to the left of the image. Between the appendage and the valve ring is a small slit-like annular defect (9 o'clock position), which represents the cause of the paravalvular leak

11.8 Case 8. Bioprosthetic Valve Dehiscence

A 74-year-old woman presented in congestive heart failure. She was known to have a history of mitral valve replacement (St. Jude Biocor #29) 1 year earlier at another hospital for *Streptococcus viridans* infective endocarditis. Her other comorbidities involved atrial fibrillation with sick sinus syndrome (necessitating pacemaker implantation), hypertension, hyperlipidemia, chronic renal insufficiency, and moderate to severe chronic lung disease.

Transthoracic echocardiography revealed mild left ventricular dysfunction and a moderate (3+) posterolateral paravalvular mitral leak in addition to severe (3–4+) tricuspid regurgitation. Blood cultures were negative on this occasion, although there was clinical concern that an infective cause of valve dehiscence was masked by recent oral antibiotic use (Figs. 11.32, 11.33, and 11.34).

She underwent redo mitral valve surgery. The surgeon noted that there was clear dehiscence of the prosthesis from the posterolateral annulus of the mitral valve, with no evidence of any active infection. As a precaution, however, the valve's original prosthesis was removed and the annulus was débrided. A 31-mm St. Jude Biocor porcine mitral valve was then sutured into place.

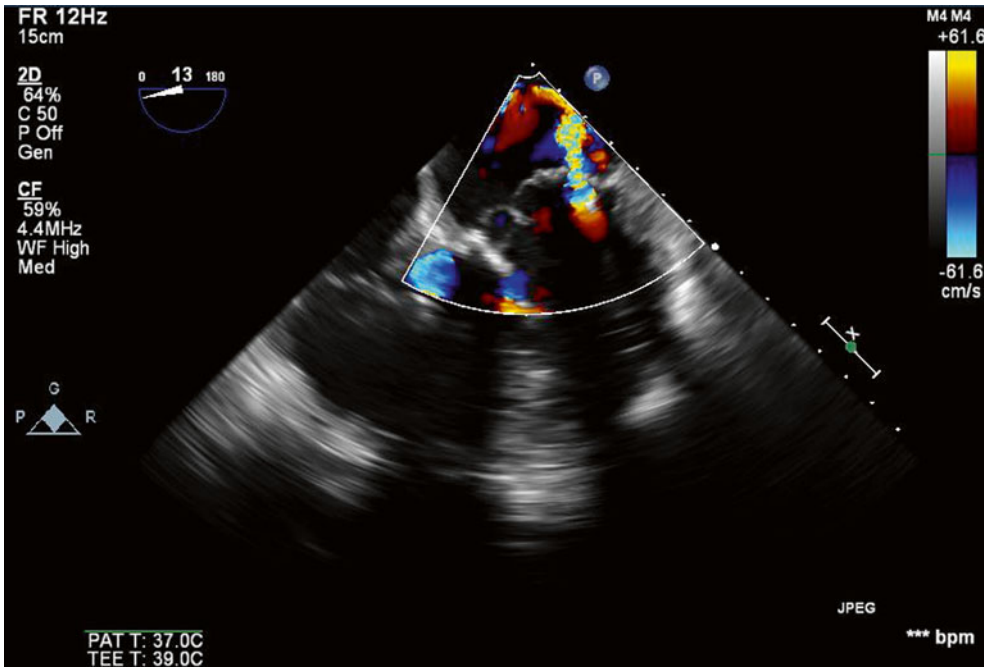

Fig. 11.32 TEE four-chamber view (13°) demonstrating a moderately severe lateral paravalvular leak on color Doppler imaging

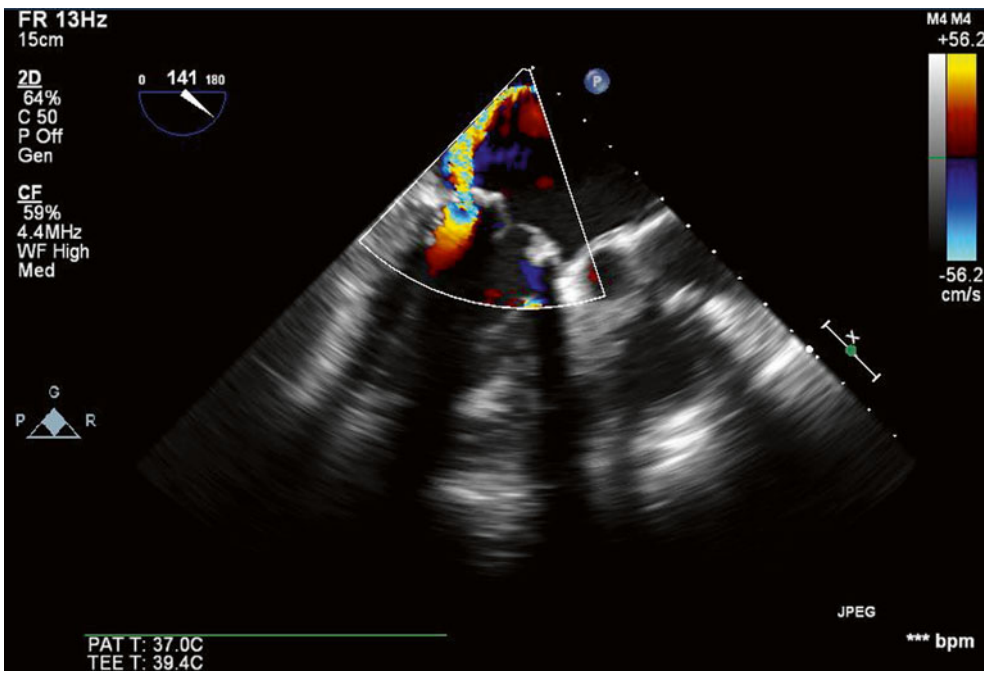

Fig. 11.33 TEE long-axis view (141°) demonstrating the same moderately severe paravalvular leak viewed more posteriorly

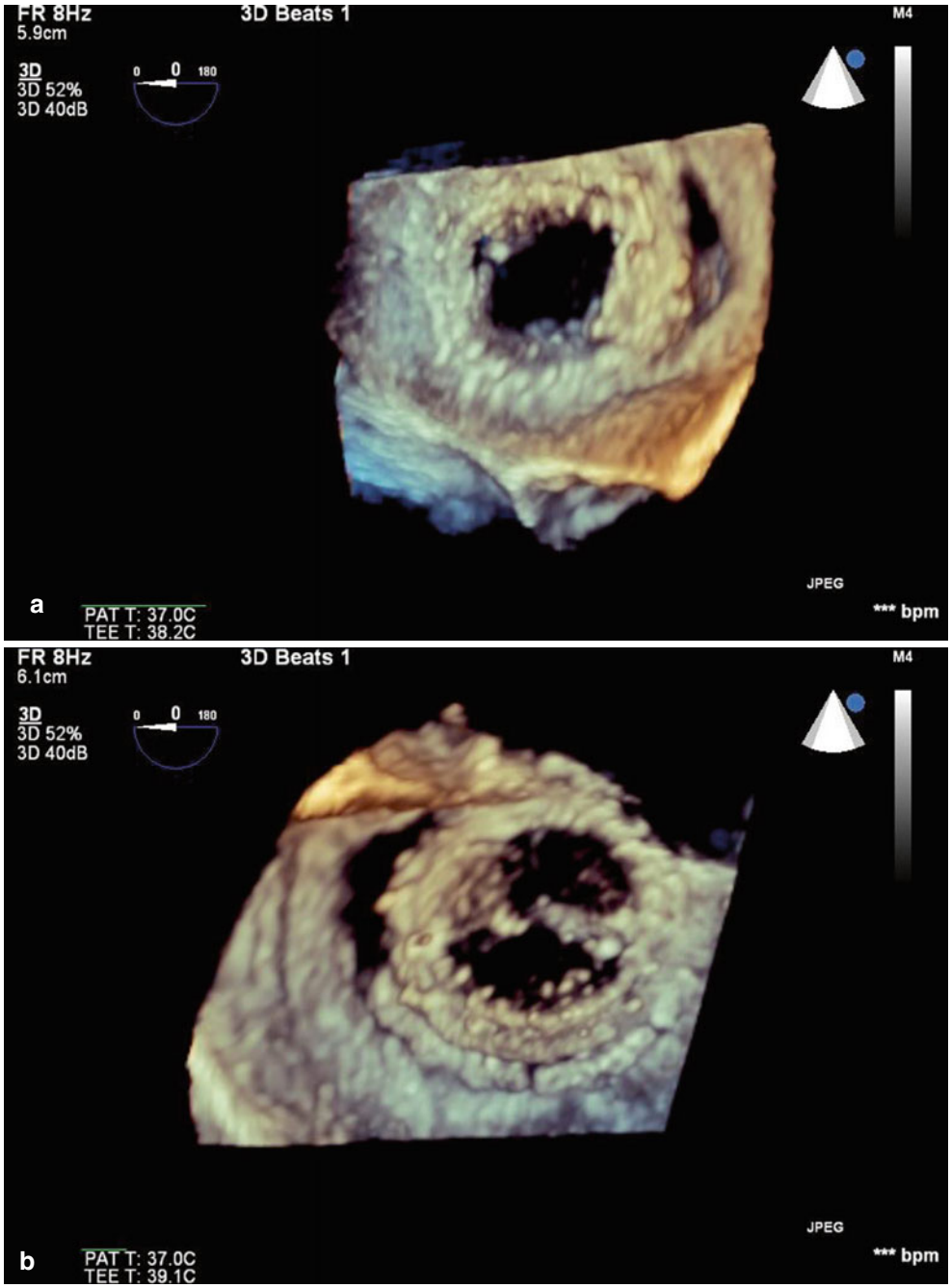

Fig. 11.34 3D reconstruction of the mitral valve viewed from the left atrium (**a**) and left ventricle (**b**). Significant dehiscence of the valve bioprosthesis is evident

11.9 Case 9. Annuloplasty Ring Dehiscence

A 58-year-old man with a history of myocardial infarction presented with symptoms of heart failure. Transthoracic echocardiography revealed severe functional ischemic mitral regurgitation, and coronary angiography revealed multivessel coronary artery disease. After extensive discussion of the risks, benefits, and alternatives, he elected to proceed with surgery. He understood that the risk of surgery was somewhat increased because of his ischemic mitral regurgitation.

He underwent coronary artery bypass grafting and insertion of a 30-mm Carpentier-McCarthy-Adams ischemic annuloplasty ring. Unfortunately, 2 years later he again started developing symptoms of heart failure. Echocardiography demonstrated significant left ventricular enlargement and dysfunction, with pulmonary hypertension and severe mitral insufficiency due to partial ring dehiscence (Figs. 11.35, 11.36, 11.37, 11.38, 11.39, 11.40, and 11.41).

Video 11.30 Parasternal long-axis view on transthoracic echocardiography (TTE), demonstrating dehiscence of the mitral annuloplasty ring, which can be seen partially hanging below the native valve within the left atrium (AVI 4432 kb)

Video 11.31 The same parasternal long-axis view with color Doppler imaging shows a severe paravalvular regurgitant jet (AVI 1942 kb)

Video 11.32 An apical four-chamber transthoracic view also shows the partially dehisced annuloplasty ring hanging below the native valve annulus in the left atrium (AVI 9310 kb)

Video 11.33 Color Doppler imaging of the same four-chamber view confirms a severe paravalvular jet laterally (AVI 2219 kb)

Video 11.34 Biplane imaging of the mitral valve at 40 and 130° on TEE also demonstrates a moderate central jet of valvular regurgitation (AVI 896 kb)

Video 11.35 3D transesophageal imaging of the mitral valve demonstrates severe dehiscence of the annuloplasty ring, involving nearly 50 % of its circumference (AVI 1046 kb)

Video 11.36 3D transesophageal imaging with color Doppler demonstrates the severe paravalvular regurgitation associated with the annuloplasty ring dehiscence (AVI 1533 kb)

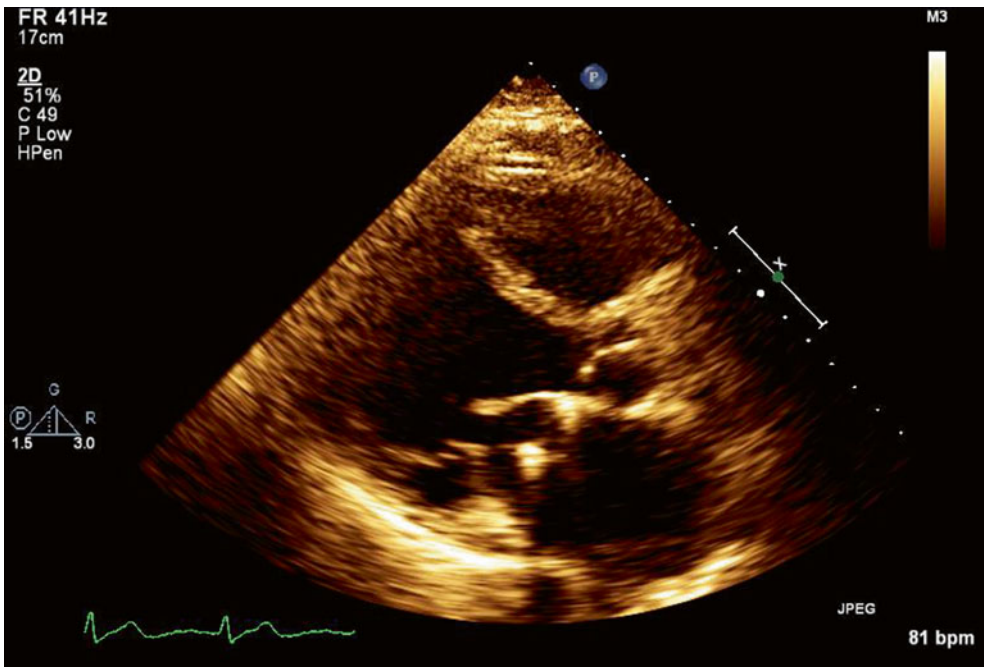

Fig. 11.35 Parasternal long-axis view on transthoracic echocardiography (TTE), demonstrating dehiscence of the mitral annuloplasty ring, which can be seen partially hanging below the native valve within the left atrium

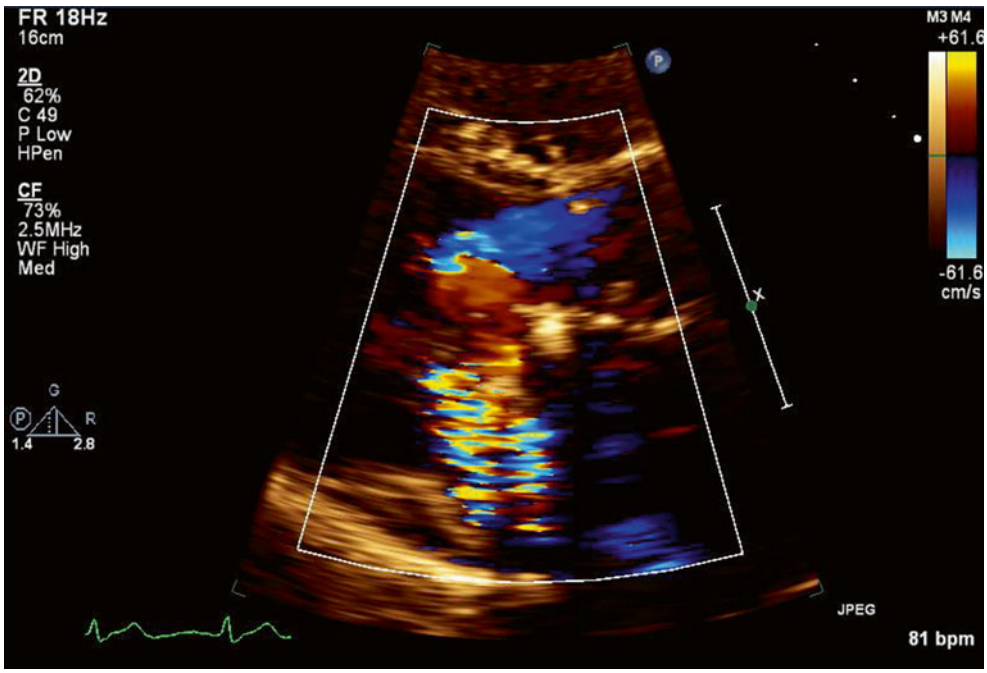

Fig. 11.36 The same parasternal long-axis view with color Doppler imaging shows a severe paravalvular regurgitant jet

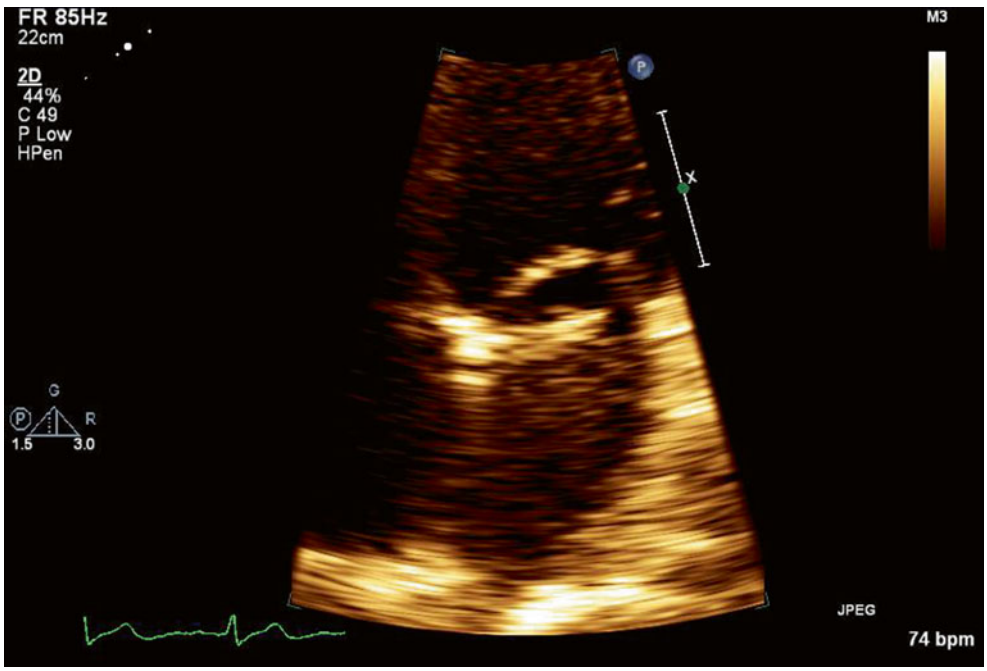

Fig. 11.37 An apical four-chamber transthoracic view also shows the partially dehisced annuloplasty ring hanging below the native valve annulus in the left atrium

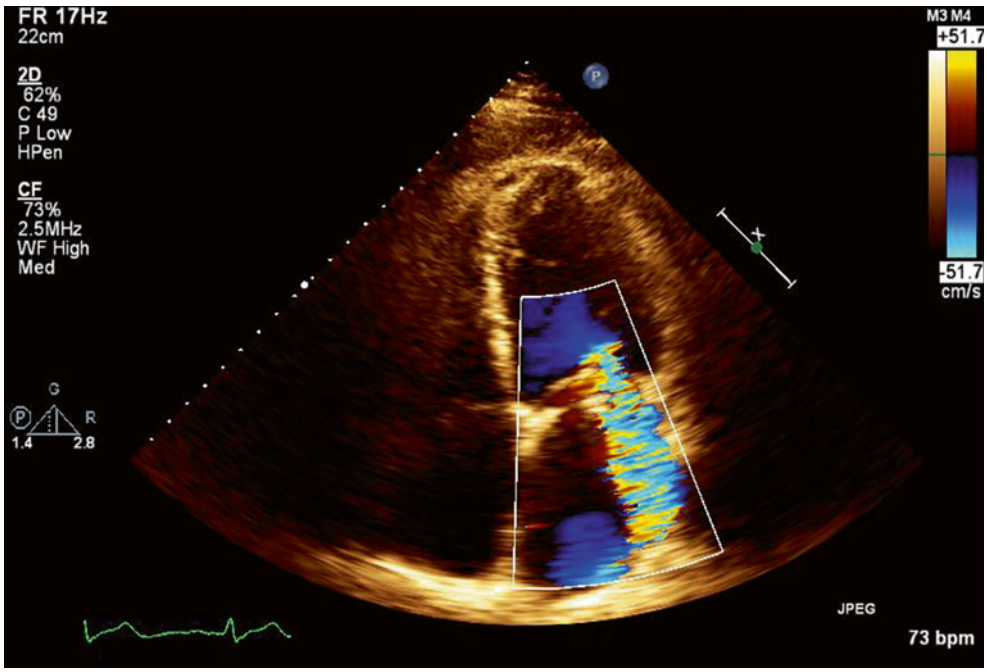

Fig. 11.38 Color Doppler imaging of the same four-chamber view confirms a severe paravalvular jet laterally

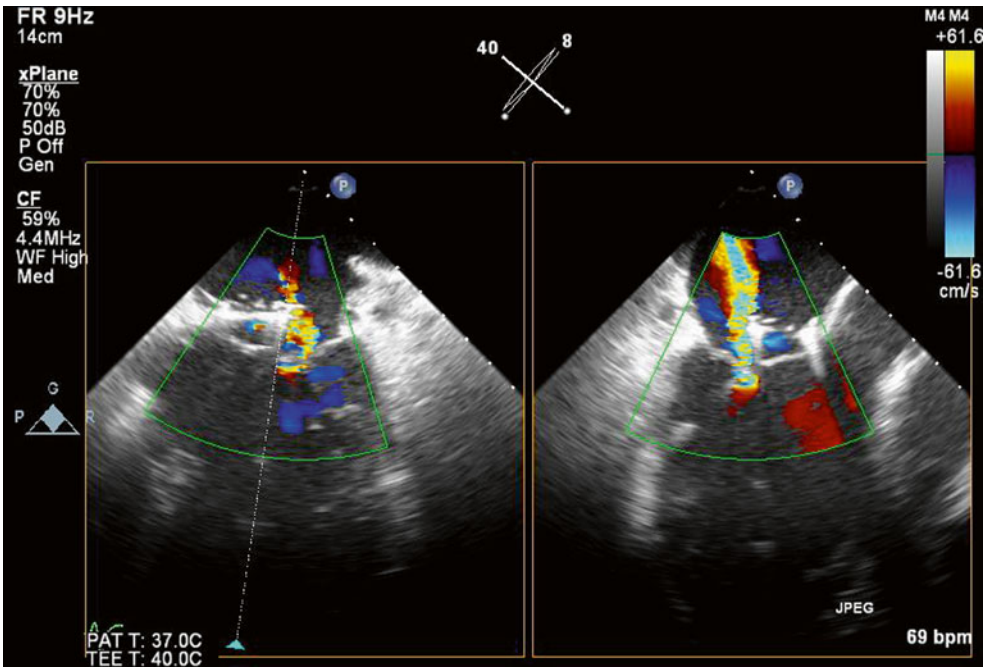

Fig. 11.39 Biplane imaging of the mitral valve at 40 and 130° on TEE also demonstrates a moderate central jet of valvular regurgitation

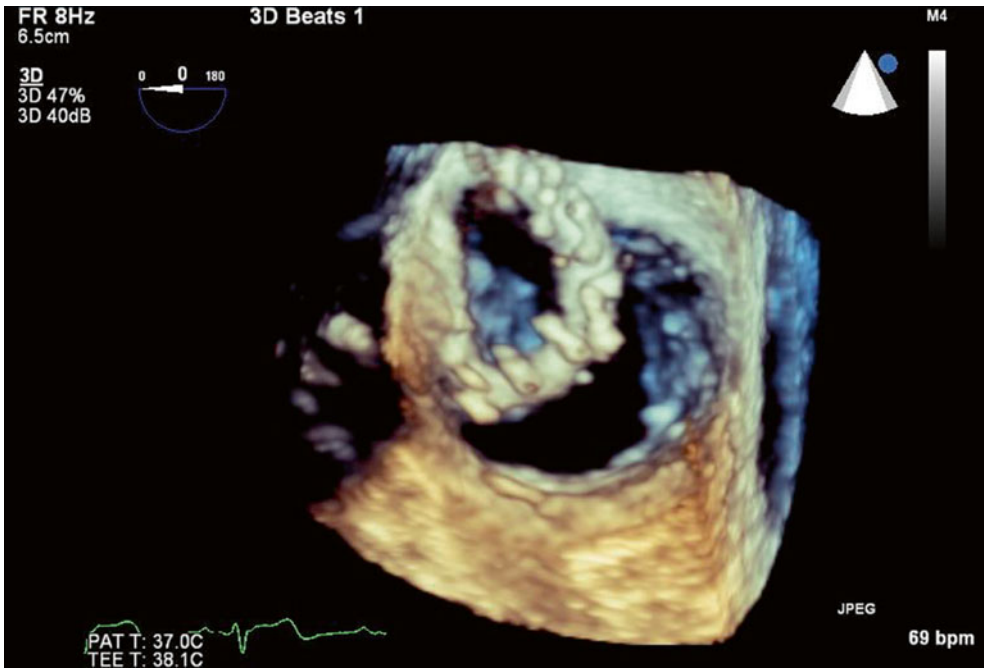

Fig. 11.40 3D transesophageal imaging of the mitral valve demonstrates severe dehiscence of the annuloplasty ring, involving nearly 50 % of its circumference

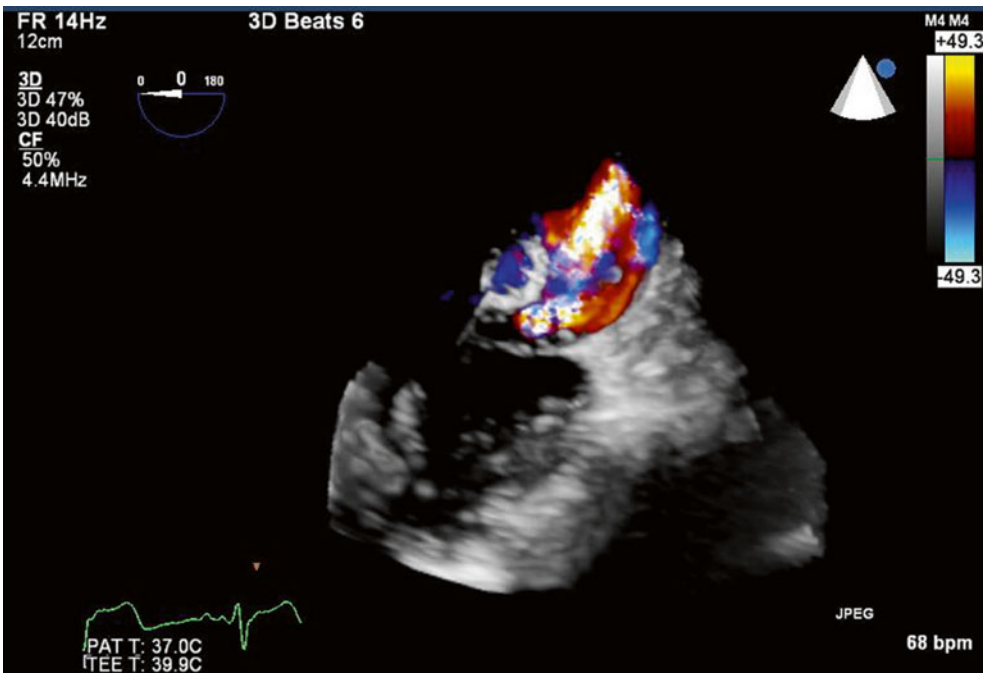

Fig. 11.41 3D transesophageal imaging with color Doppler demonstrates the severe paravalvular regurgitation associated with the annuloplasty ring dehiscence

11.10 Case 10. Inflammatory Response

A 51-year-old man with a history of mitral valve repair (35-mm Duran annuloplasty ring) for mitral valve prolapse 2 years earlier (Figs. 11.42, 11.43, 11.44, 11.45, and 11.46) presented with a transient ischemic attack and severe mitral stenosis. The peak and mean transvalvular gradients measured 23 mmHg and 14 mmHg respectively. Transesophageal echocardiography demonstrated the mitral annulus to be severely thickened globally (0.6 cm), with laminated echogenic material extending from the annulus onto both leaflet bodies (Figs. 11.47, 11.48, 11.49, 11.50, 11.51, and 11.52). This thickening severely restricted the valve orifice and leaflet opening. The appearance was felt to be suspicious for infective endocarditis or laminar thrombus, although he denied any constitutional symptoms suggestive of infection. Multiple blood cultures remained negative.

He was commenced on empiric antibiotic therapy and therapeutically anticoagulated with heparin prior to redo mitral valve surgery. The ring and adjacent tissue was resected and a mechanical mitral valve was sutured in place. Histology revealed extensive inflammatory response with no evidence of thrombus or infection.

Video 11.37 Transesophageal view (at 91°) of the repaired mitral valve with an annuloplasty ring in situ, taken immediately after the original valve surgery. There is good leaflet coaptation without restriction of leaflet movement (AVI 4700 kb)

Video 11.38 Another transesophageal view (at 139°) taken immediately after the original valve surgery, showing good leaflet coaptation without restriction of leaflet movement (AVI 4752 kb)

Video 11.39 Color Doppler imaging at the same transesophageal 139° view immediately after the original valve repair confirms that there was no residual regurgitation (AVI 1148 kb)

Video 11.40 A TEE image (0°) obtained 2 years later showed that the mitral annulus was severely thickened circumferentially, with laminated echogenic material extending from the annulus onto both leaflet bodies. This thickening restricted leaflet opening and resulted in a small, stenotic valve orifice (AVI 3941 kb)

Video 11.41 TEE view at 60°, also obtained 2 years later, showing thickening of the mitral annulus (AVI 5445 kb)

Video 11.42 TEE view at 90°, also obtained 2 years later, showing thickening of the mitral annulus (AVI 5005 kb)

Video 11.43 TEE view at 120°, also obtained 2 years later, showing thickening of the mitral annulus (AVI 3815 kb)

Video 11.44 3D imaging of the mitral valve demonstrated a significant reduction in valve orifice area related to the smooth, laminated echogenic material overlying the annuloplasty ring and extending onto the leaflet bases. Severe associated valve leaflet thickening was also evident (AVI 681 kb)

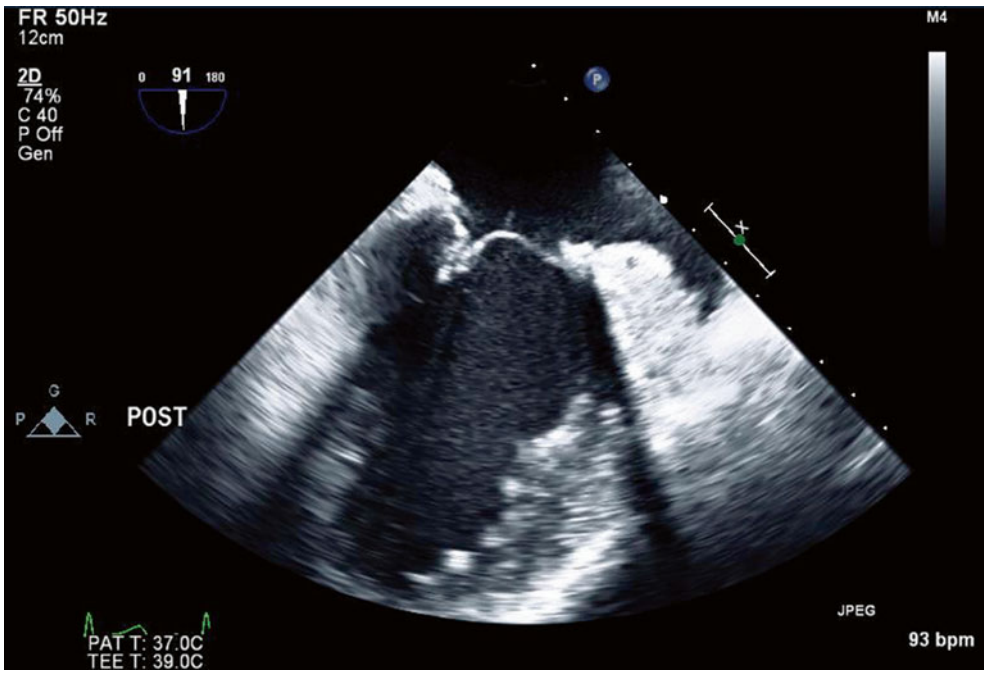

Fig. 11.42 Transesophageal view (91°) of the repaired mitral valve with an annuloplasty ring in situ, taken immediately after the original valve surgery. There is good leaflet coaptation without restriction of leaflet movement

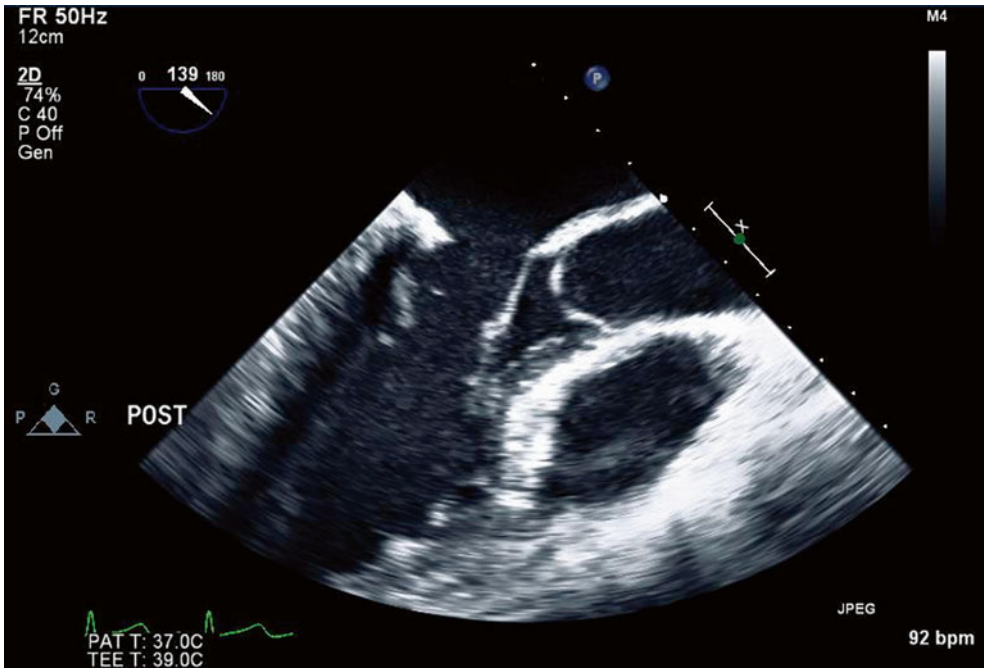

Fig. 11.43 Another transesophageal view (139°) taken immediately after the original valve surgery. There is good leaflet coaptation without restriction of leaflet movement

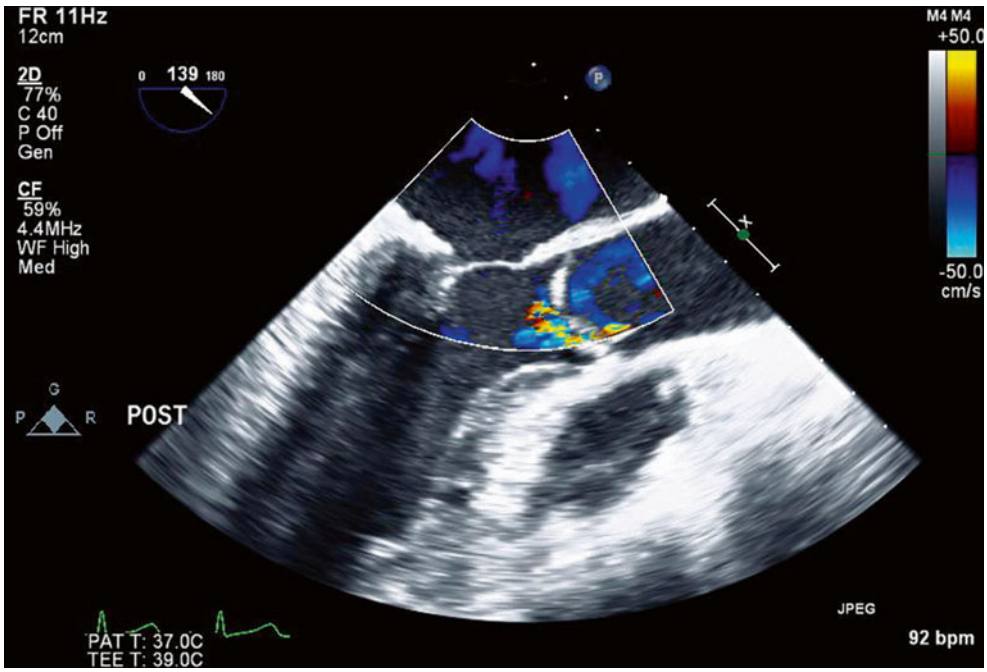

Fig. 11.44 Color Doppler imaging at the same transesophageal 139° view immediately after the original valve repair confirms that there was no residual regurgitation

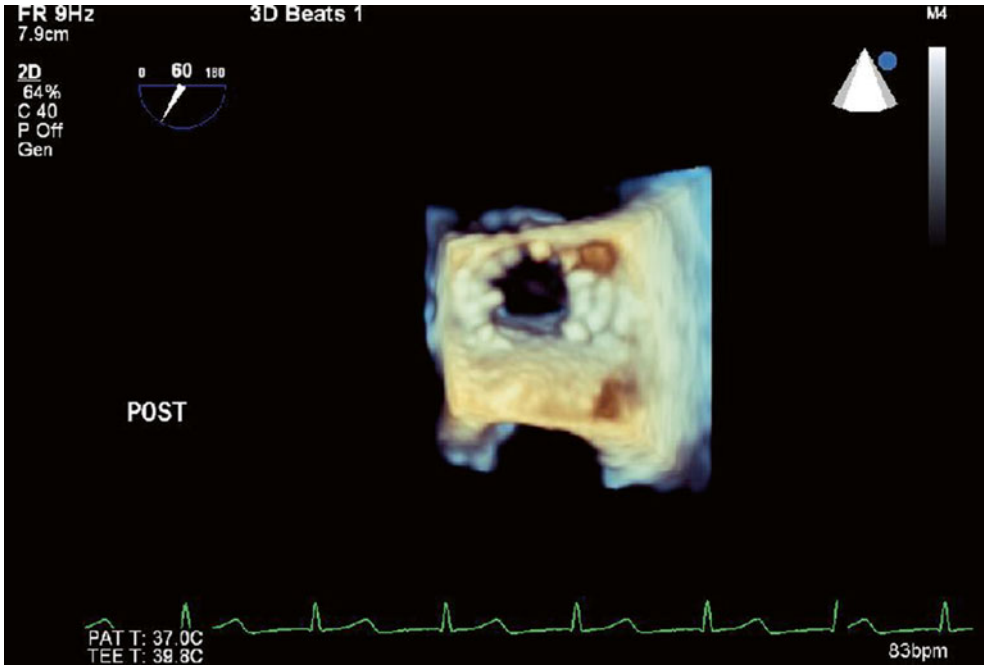

Fig. 11.45 3D imaging immediately after the original valve repair confirms good leaflet excursion with a normal-sized valve orifice area during diastole

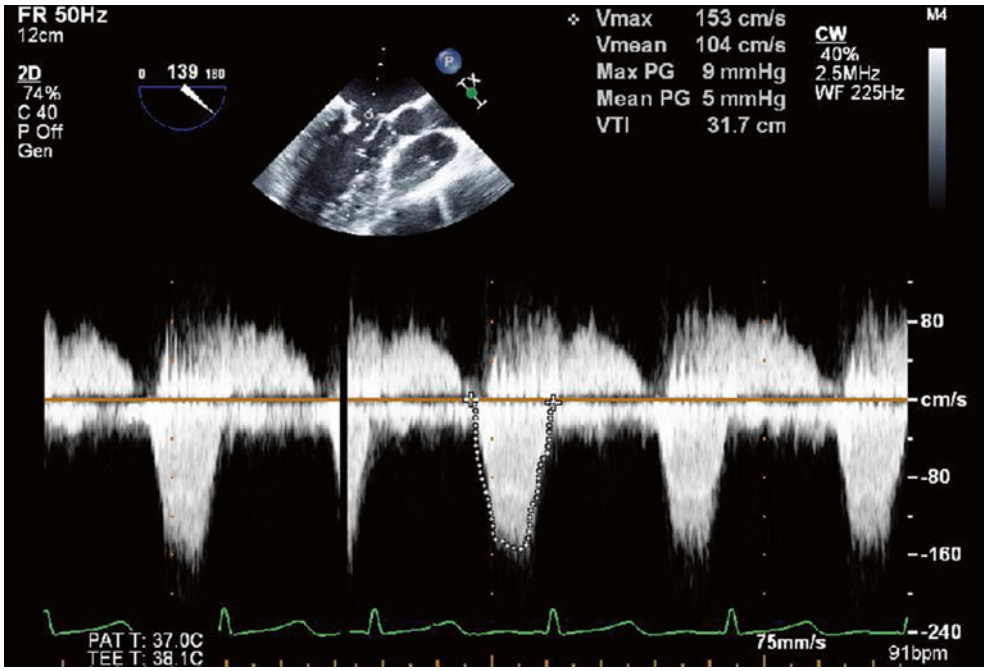

Fig. 11.46 Transvalvular gradients immediately after the original valve repair were within acceptable limits, with a peak gradient of 9 mmHg and a mean gradient of 5 mmHg

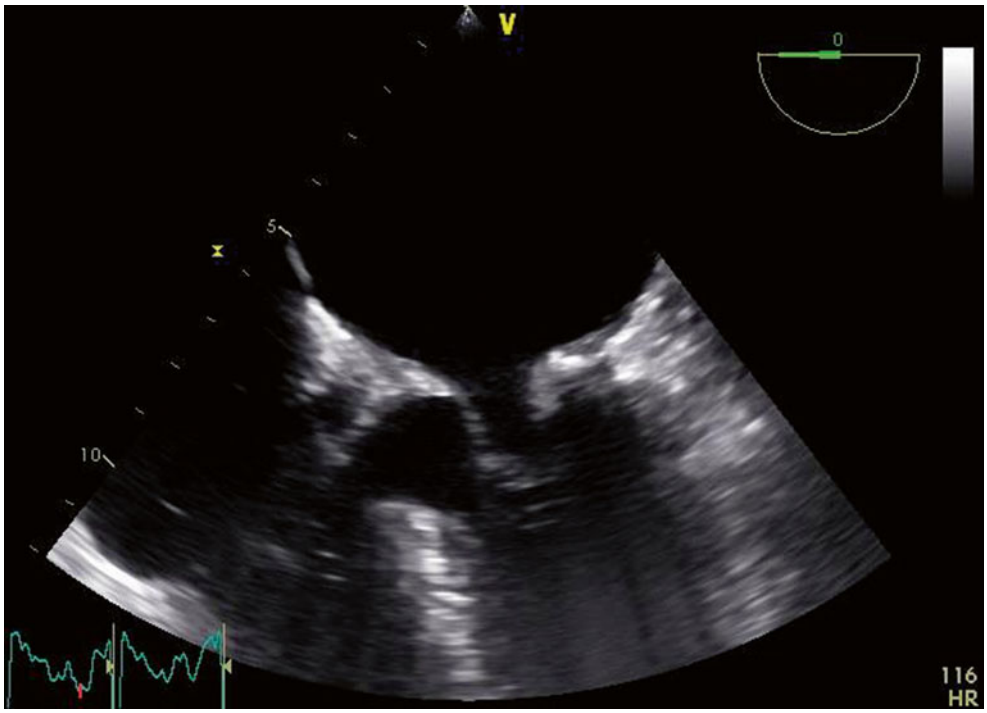

Fig. 11.47 A TEE image (0°) obtained 2 years later showed that the mitral annulus was severely thickened circumferentially, with laminated echogenic material extending from the annulus onto both leaflet bodies. This thickening restricted leaflet opening and resulted in a small, stenotic valve orifice

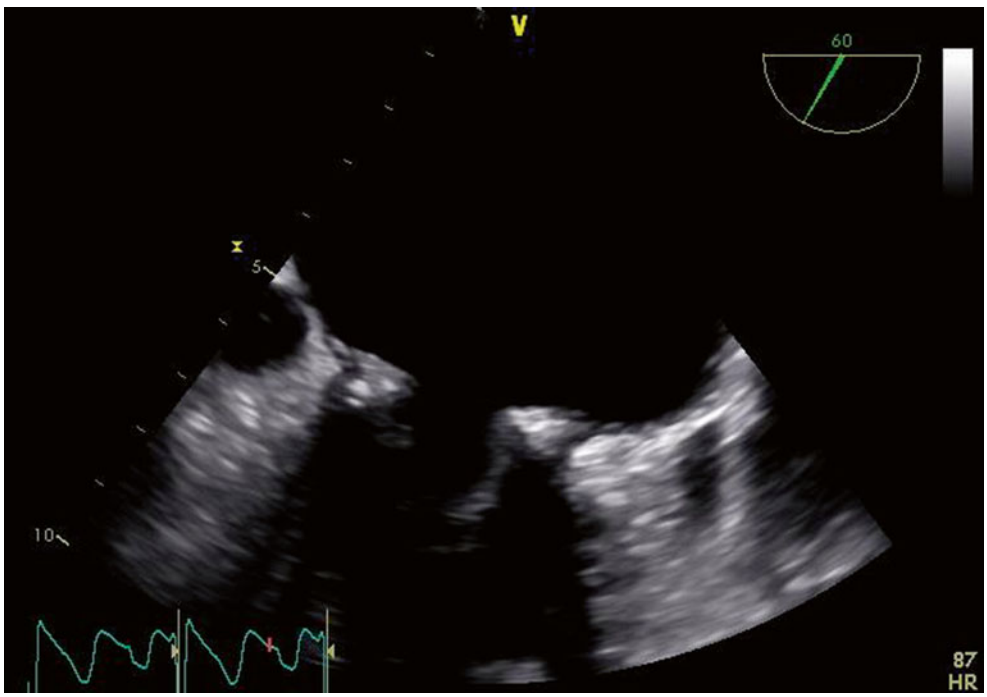

Fig. 11.48 TEE view at 60° also obtained 2 years later, showing thickening of the mitral annulus

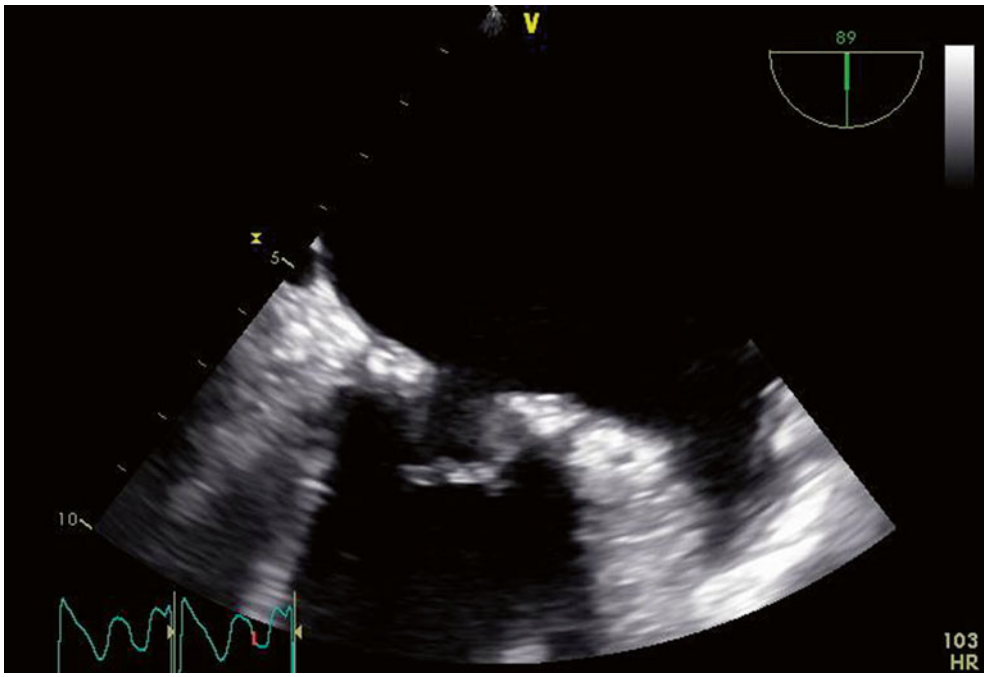

Fig. 11.49 TEE view at 90° also obtained 2 years later, showing thickening of the mitral annulus

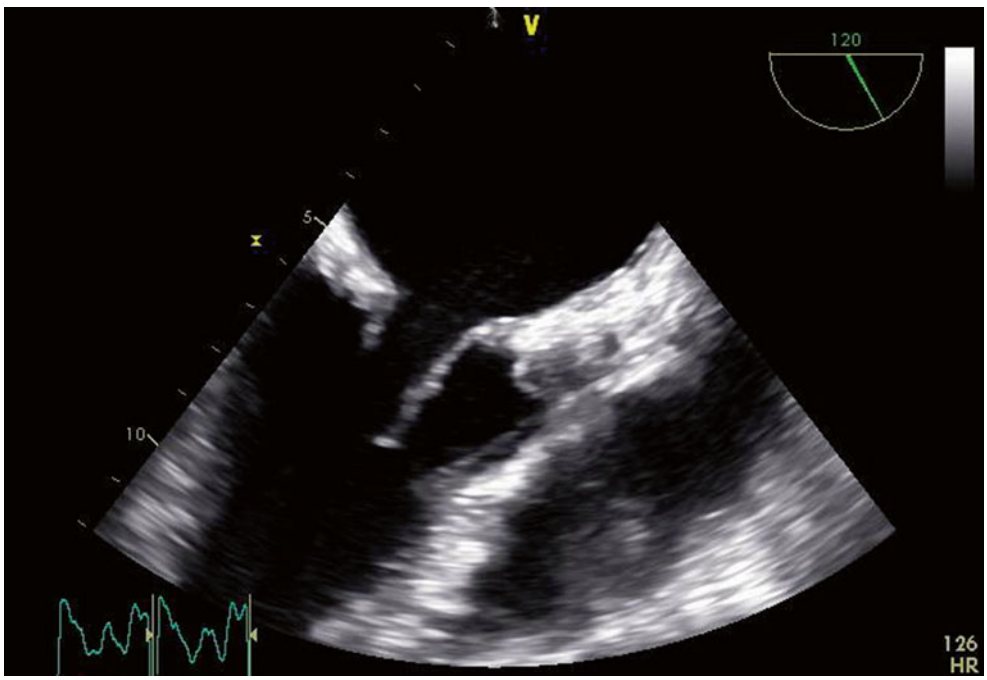

Fig. 11.50 TEE view at 120° also obtained 2 years later, showing thickening of the mitral annulus

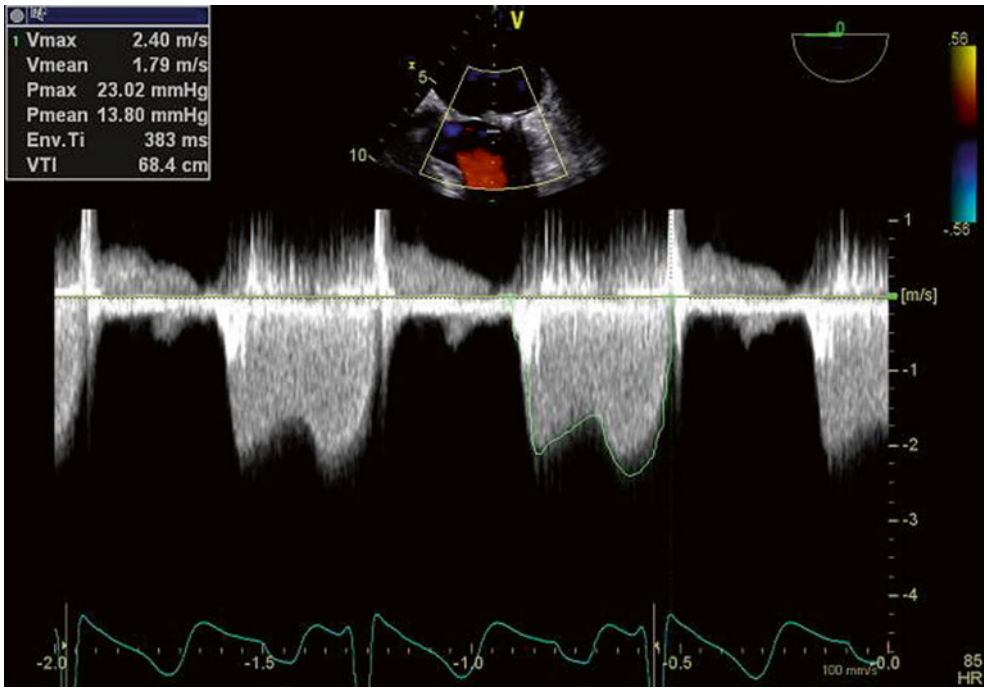

Fig. 11.51 A significant interval increase in transvalvular gradients was noted, to peak and mean gradients of 23 and 14 mmHg respectively

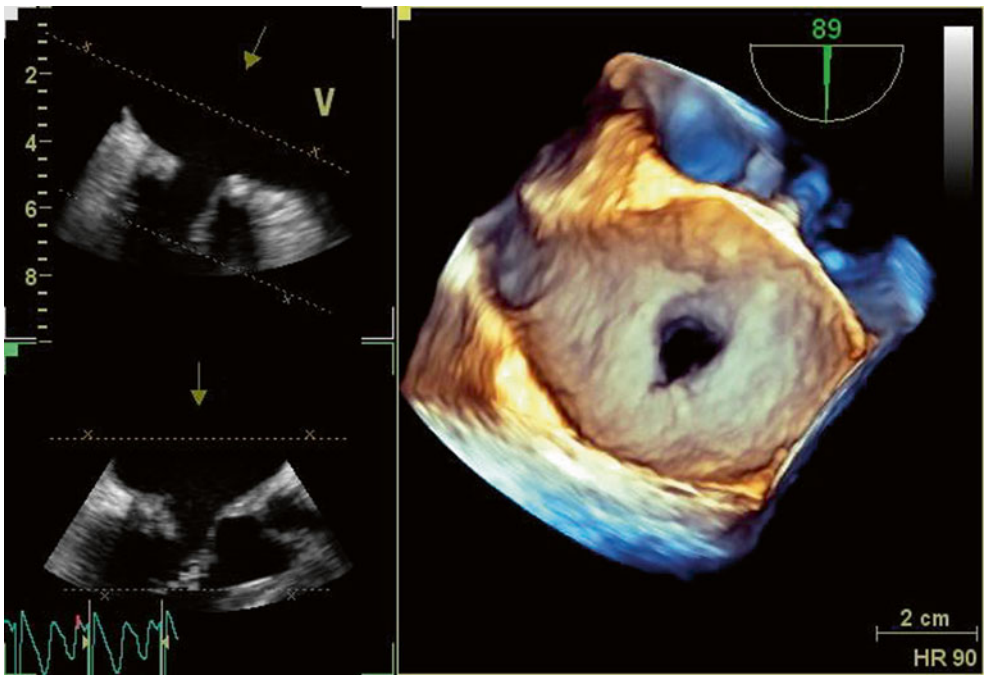

Fig. 11.52 3D imaging of the mitral valve demonstrated a significant reduction in valve orifice area related to the smooth, laminated echogenic material overlying the annuloplasty ring and extending onto the leaflet bases. Severe associated valve leaflet thickening was also evident

11.11 Case 11. Inflammatory Response

A 60-year-old woman was noted to have a new murmur, shortness of breath, and fatigue when presenting for routine cardiology review. She denied any constitutional symptoms, including fever, diaphoresis, or change in weight. Three months earlier she had undergone a mitral valve repair for severe symptomatic mitral regurgitation secondary to prolapse (Fig. 11.53).

She underwent a transesophageal echocardiogram, which demonstrated multiple mobile echodensities attached to the left atrial aspect of the mitral valve annuloplasty prosthesis, with suggestion of abscess formation along the intervalvular fibrosa and a small (0.6 cm, Qp:Qs 1.1) Gerbode-type defect (left ventricle to right atrial shunt) without evidence of right ventricular volume overload (Figs. 11.54, 11.55, 11.56, 11.57, and 11.58).

The appearance was felt to be concerning for vegetations or thrombi. She underwent cardiac surgery with resection of the previous annuloplasty ring, insertion of a bioprosthetic mitral valve replacement, and closure of the Gerbode defect. Histological assessment of the resected tissue revealed extensive chronic inflammation with a small amount of acute fibrinous exudate. No microorganisms or organized thrombi were identified.

On routine review 6 months later, she remained well, with no symptoms of heart failure or constitutional symptoms including fever, but repeat echocardiography again demonstrated multiple echodensities attached to the new valve prosthesis (Figs. 11.59 and 11.60). In view of her stable clinical status, it was felt that these new abnormalities represented a further inflammatory response to another valve prosthesis. She was managed conservatively with ongoing discussion regarding the need for therapeutic anticoagulation.

Video 11.45 Normal TEE (119° long-axis view) of the first bioprosthetic valve immediately after replacement (AVI 7356 kb)

Video 11.46 Standard TEE (0° view) demonstrating extensive multiple mobile echodensities attached to the left atrial aspect of the valve leaflets and annulus (AVI 8015 kb)

Video 11.47 Standard TEE (61° view) demonstrating extensive multiple mobile echodensities attached to the left atrial aspect of the valve leaflets and annulus (AVI 6522 kb)

Video 11.48 Standard TEE (94° view) demonstrating extensive multiple mobile echodensities attached to the left atrial aspect of the valve leaflets and annulus (AVI 6563 kb)

Video 11.49 Biplane 0/90° view demonstrating orthogonal views of the mitral valve prosthesis with multiple mobile echodensities attached (AVI 4399 kb)

Video 11.50 3D reconstruction of the mitral valve prosthesis with multiple mobile echodensities attached to the valve annulus and leaflets (AVI 1340 kb)

Video 11.51 Repeat TEE after the redo bioprosthetic mitral valve replacement also demonstrated small, mobile echodensities adherent to the left atrial aspect of the prosthetic valve annulus (AVI 7291 kb)

Video 11.52 Repeat TEE after the redo bioprosthetic mitral valve replacement also demonstrated small, mobile echodensities adherent to the left atrial aspect of the prosthetic valve annulus (AVI 3147 kb)

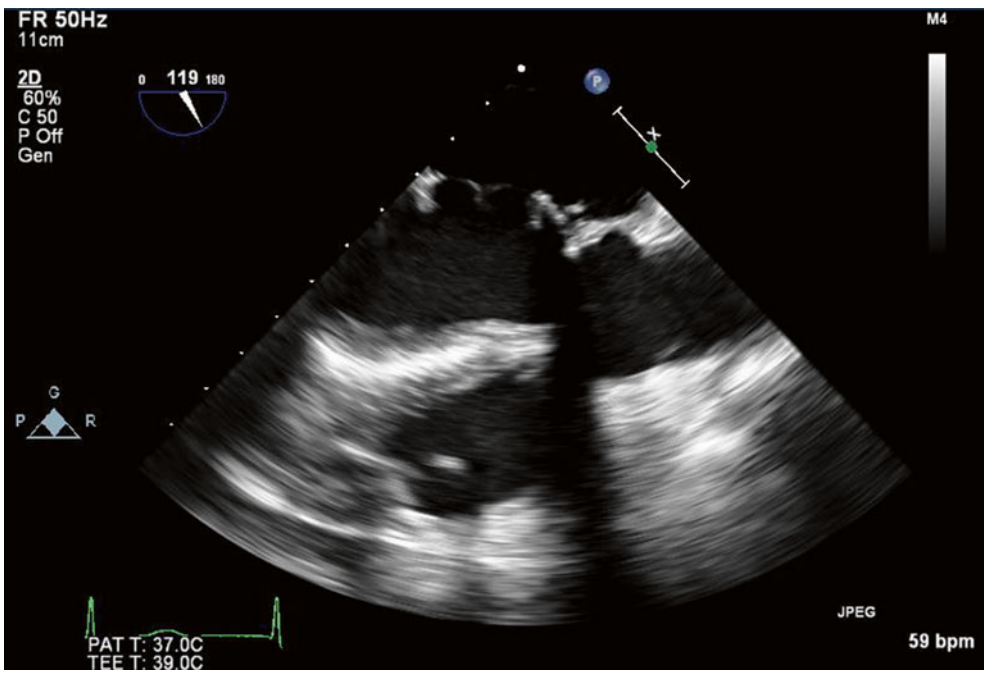

Fig. 11.53 Normal TEE (119° long-axis view) of the first bioprosthetic valve immediately after replacement

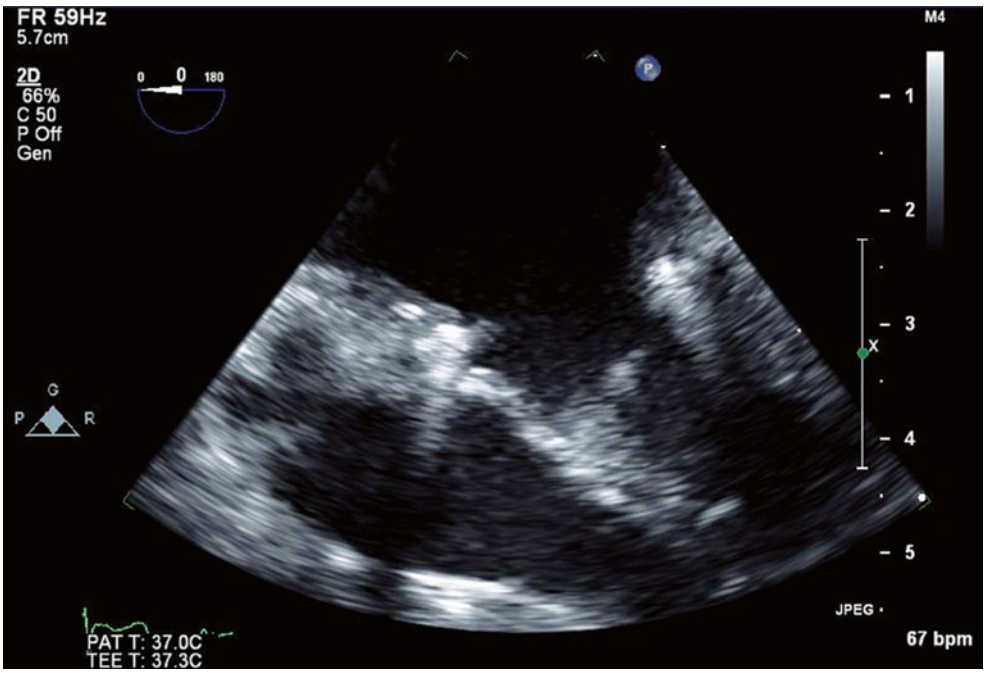

Fig. 11.54 Standard TEE (0° view) demonstrating extensive multiple mobile echodensities attached to the left atrial aspect of the valve leaflets and annulus

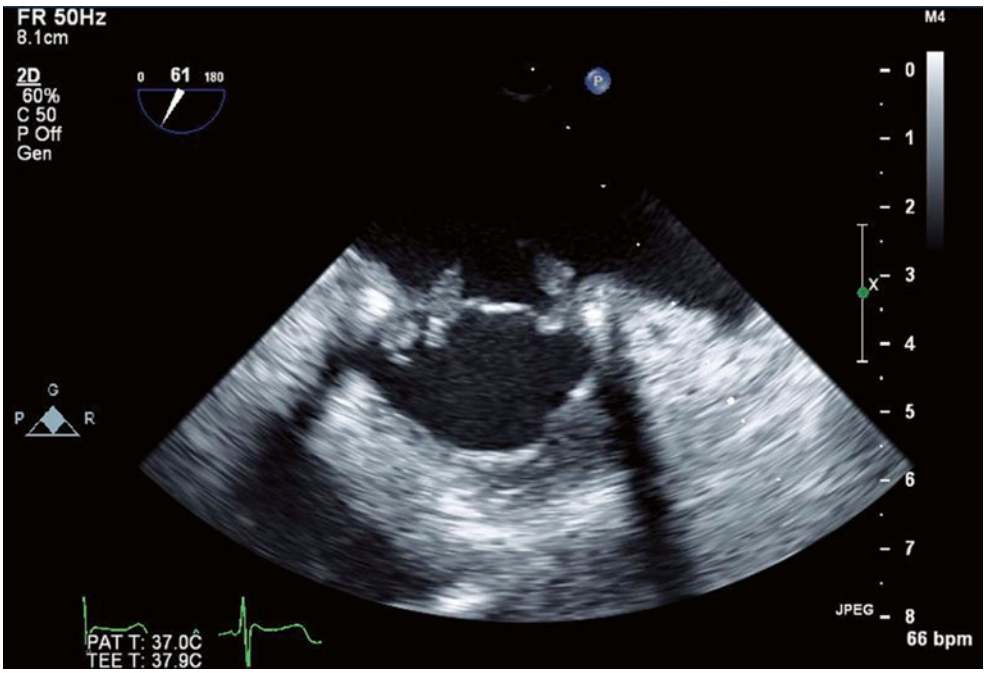

Fig. 11.55 Standard TEE (61° view) demonstrating extensive multiple mobile echodensities attached to the left atrial aspect of the valve leaflets and annulus

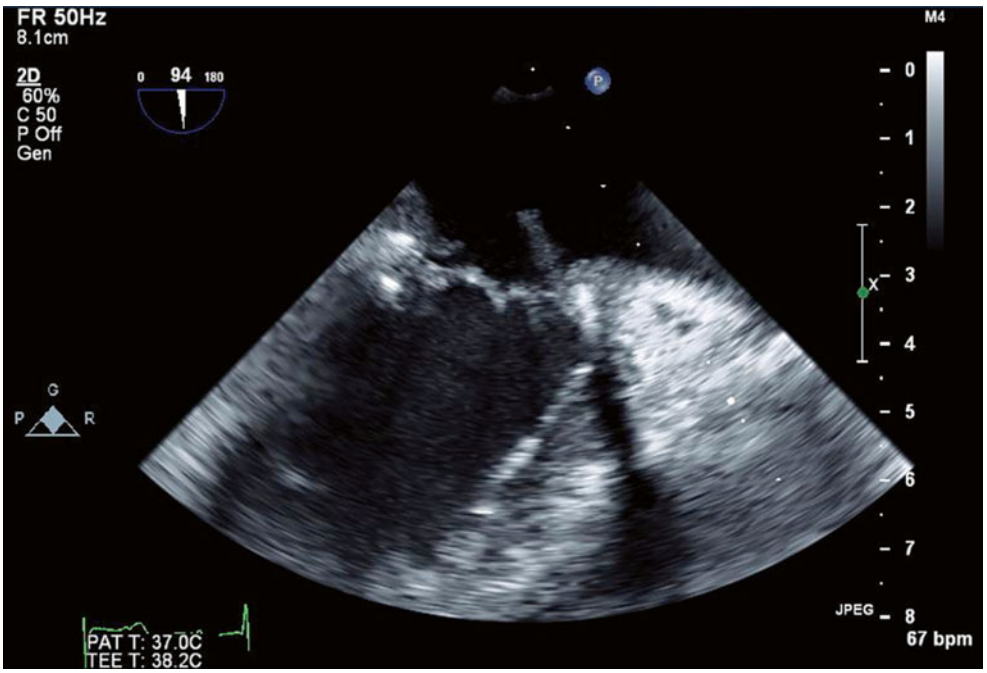

Fig. 11.56 Standard TEE (94° view) demonstrating extensive multiple mobile echodensities attached to the left atrial aspect of the valve leaflets and annulus

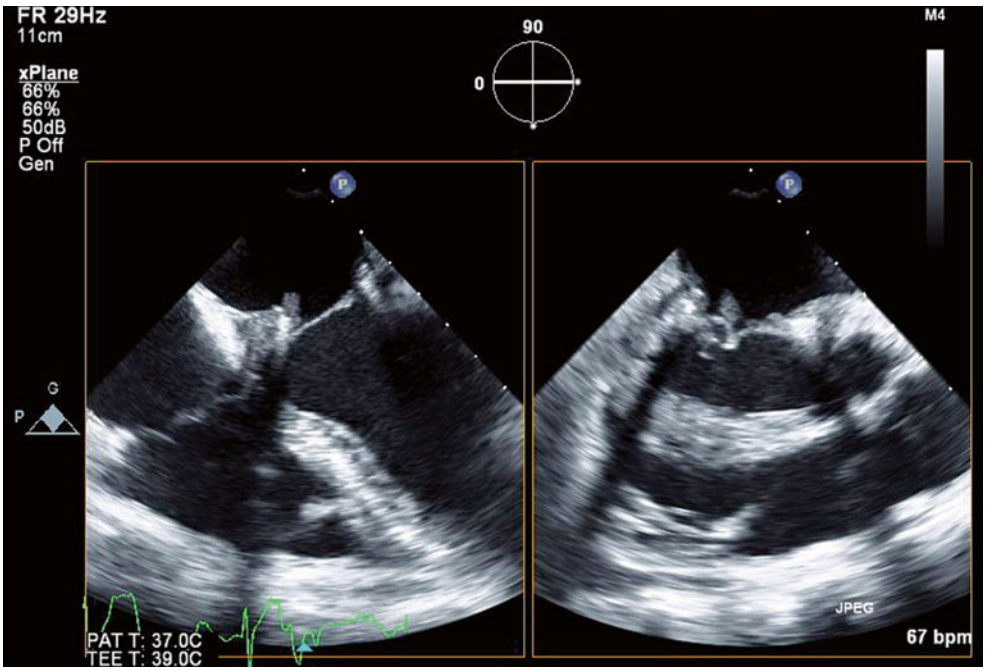

Fig. 11.57 Biplane 0/90° view demonstrating orthogonal views of the mitral valve prosthesis with multiple mobile echodensities attached

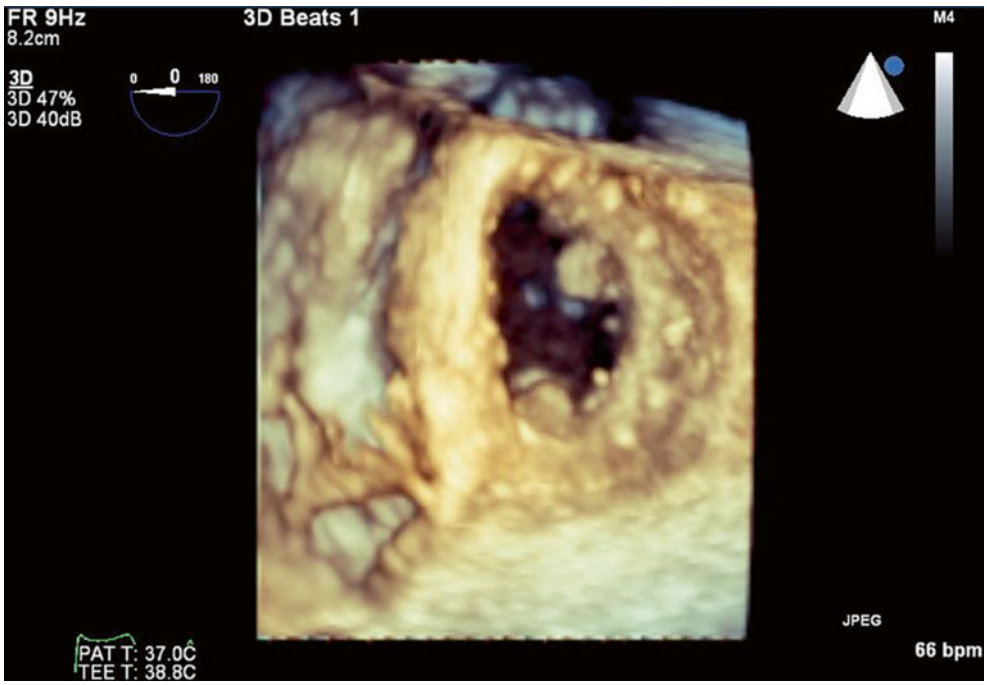

Fig. 11.58 3D reconstruction of the mitral valve prosthesis with multiple mobile echodensities attached to the valve annulus and leaflets

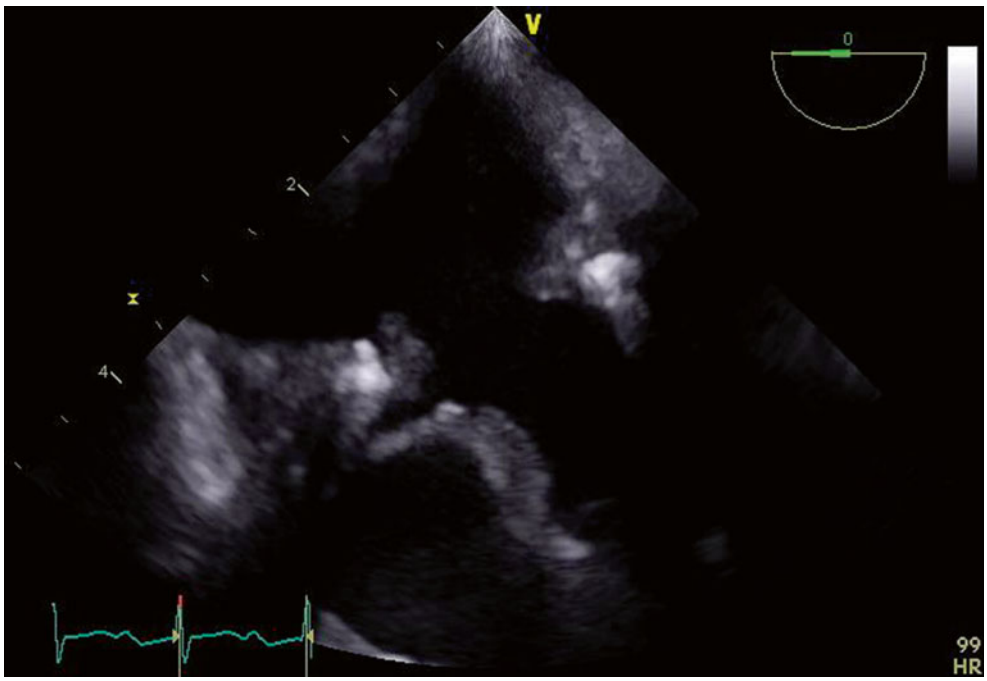

Fig. 11.59 Repeat TEE after the redo bioprosthetic mitral valve replacement also demonstrated small, mobile echodensities adherent to the left atrial aspect of the prosthetic valve annulus

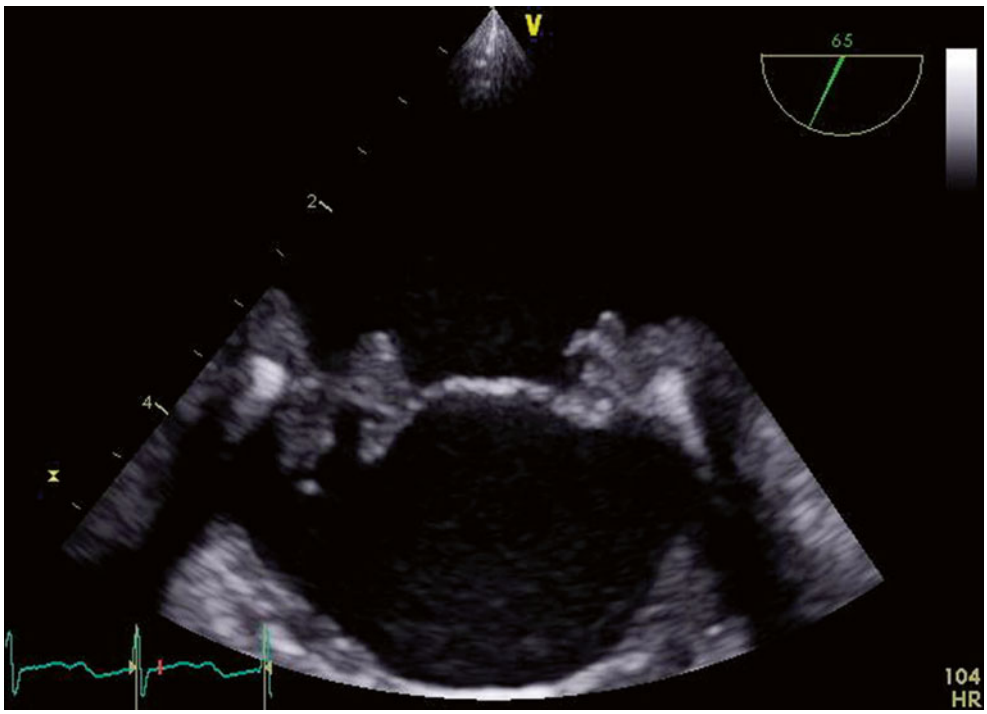

Fig. 11.60 Repeat TEE after the redo bioprosthetic mitral valve replacement also demonstrated small, mobile echodensities adherent to the left atrial aspect of the prosthetic valve annulus

11.12 Case 12. Mitral Valve Prosthesis Thrombus

A 72-year-old woman with a history of rheumatic heart disease, obstructive lung disease, hypertension, and chronic kidney disease underwent a third-time redo double valve replacement involving a mitral valve replacement (27-mm Biocor bioprosthesis), aortic root replacement with reimplantation of the coronary arteries, an aortic valve replacement (25-mm Freestyle bioprosthesis), and ascending aorta graft repair. The redo mitral valve replacement had required extensive annular débridement and reconstruction of the fibrous skeleton of the heart with pericardial patches because of heavy calcification. The postoperative period was complicated by shock requiring arteriovenous extracorporeal membrane oxygenation support. Thrombus formation within the left atrium involved the mitral valve prosthesis, and she was returned to surgery for urgent thrombectomy of the mitral valve. Layered thrombus was found within the left atrium, which extended across the mitral valve and impeded its opening (Figs. 11.61, 11.62, 11.63, 11.64, 11.65, 11.66, 11.67, 11.68, and 11.69).

Video 11.53 3D reconstruction of the mitral valve immediately after initial implantation, demonstrating a normal, functioning valve (AVI 996 kb)

Video 11.54 Two days after surgery, while the patient was on arteriovenous extracorporeal membrane oxygenation support, TEE (0° view) demonstrated severe biventricular dysfunction and severe mitral valve dysfunction. Both leaflets demonstrated very poor mobility and were severely restricted by overlying thrombus, which extended into the left atrium. Swirling sludge could be seen throughout the left atrium. The left atrial appendage had been ligated at the time of the original surgery (AVI 7260 kb)

Video 11.55 TEE (138° view) performed at the same time as Video 11.54 also demonstrated severe biventricular dysfunction and severe mitral valve dysfunction. Both leaflets demonstrated very poor mobility and were severely restricted by overlying thrombus, which extended into the left atrium. Swirling sludge could be seen throughout the left atrium (AVI 7232 kb)

Video 11.56 Color Doppler imaging demonstrated only a small jet of turbulent forwards flow across the severely stenotic mitral valve (AVI 2125 kb)

Video 11.57 3D reconstruction of the mitral valve showed a severely stenotic valve with only a slit-like valve orifice remaining (AVI 1136 kb)

Video 11.58 After the thrombectomy, leaflet mobility improved, but a degree of restricted leaflet excursion persisted because of residual thrombus on the valve leaflets and annulus. Biventricular function remained severely impaired (AVI 3627 kb)

Video 11.59 Zoomed view of Video 11.58 (AVI 5439 kb)

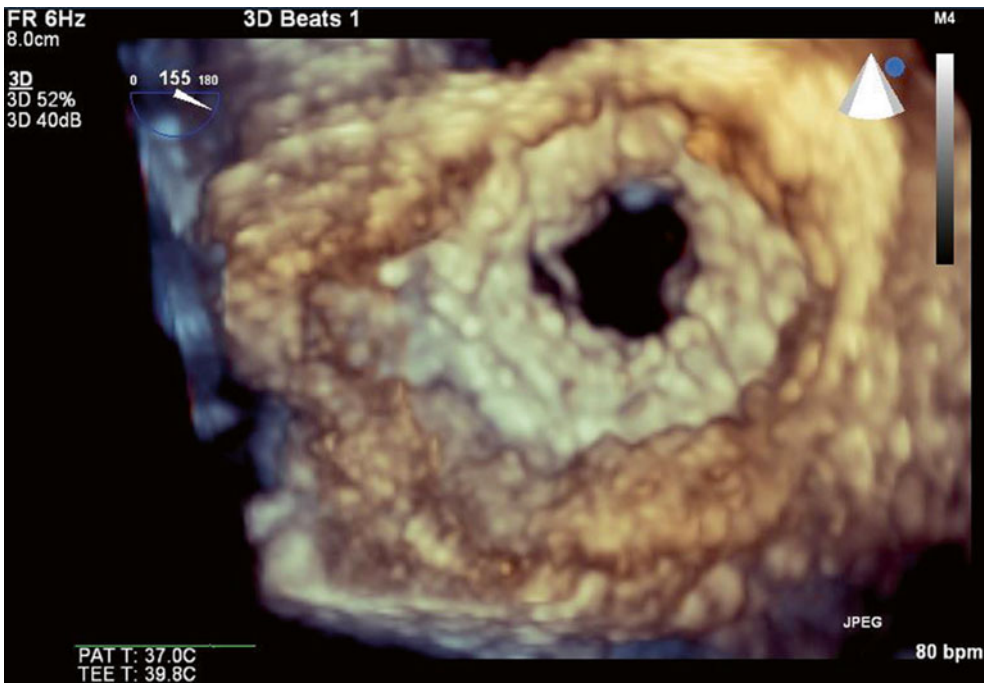

Fig. 11.61 3D reconstruction of the mitral valve immediately after initial implantation, demonstrating a normal, functioning valve

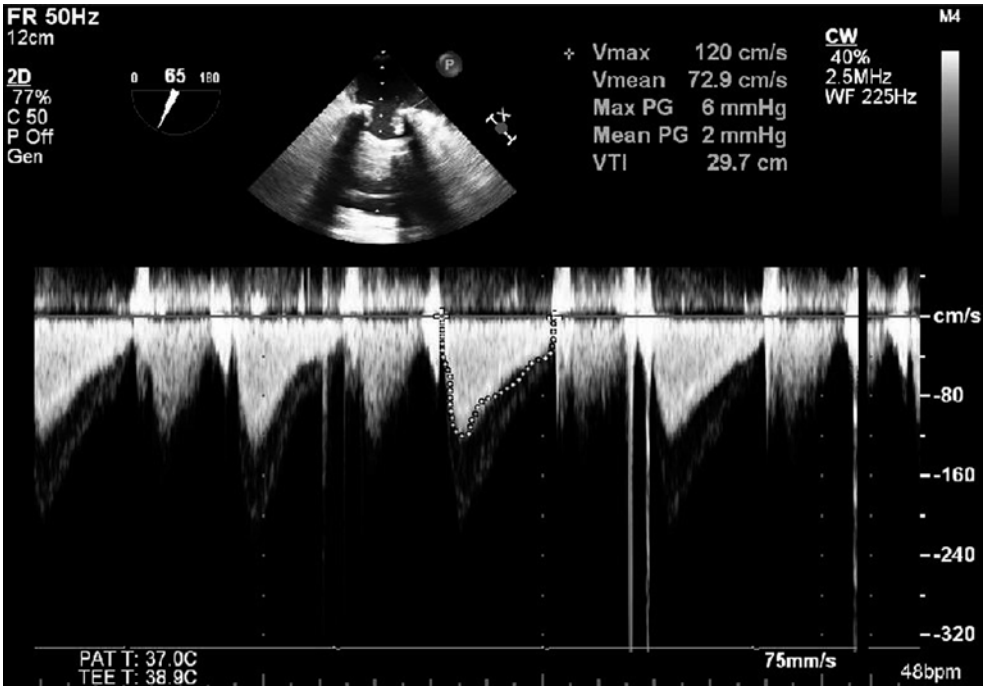

Fig. 11.62 Peak transvalvular gradient (6 mmHg) and mean transvalvular gradient (2 mmHg) immediately after implantation

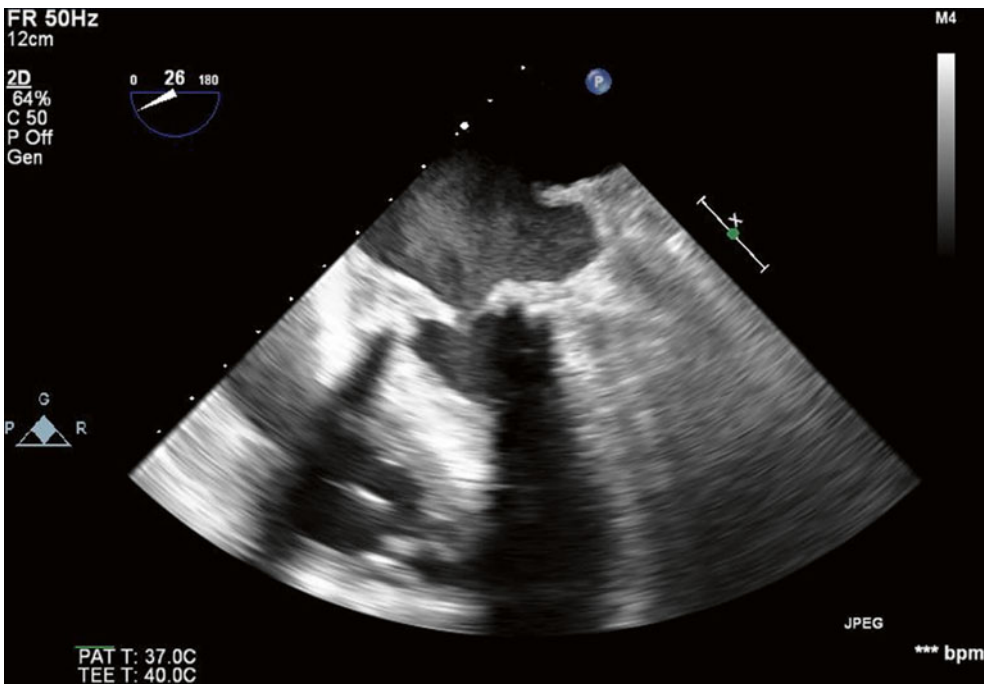

Fig. 11.63 Two days after surgery, while the patient was on arteriovenous extracorporeal membrane oxygenation support, TEE (0° view) demonstrated severe biventricular dysfunction and severe mitral valve dysfunction. Both leaflets demonstrated very poor mobility and were severely restricted by overlying thrombus, which extended into the left atrium. Swirling sludge could be seen throughout the left atrium. The left atrial appendage had been ligated at the time of the original surgery

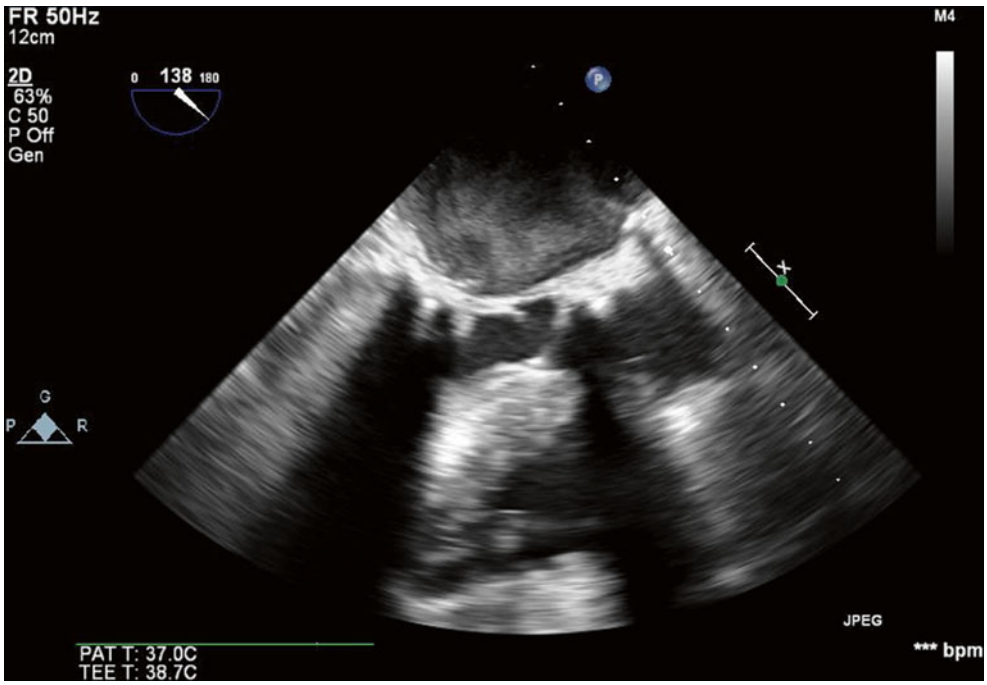

Fig. 11.64 TEE (138° view) performed at the same time as Fig. 11.63 also demonstrated severe biventricular dysfunction and severe mitral valve dysfunction. Both leaflets demonstrated very poor mobility and were severely restricted by overlying thrombus, which extended into the left atrium. Swirling sludge could be seen throughout the left atrium

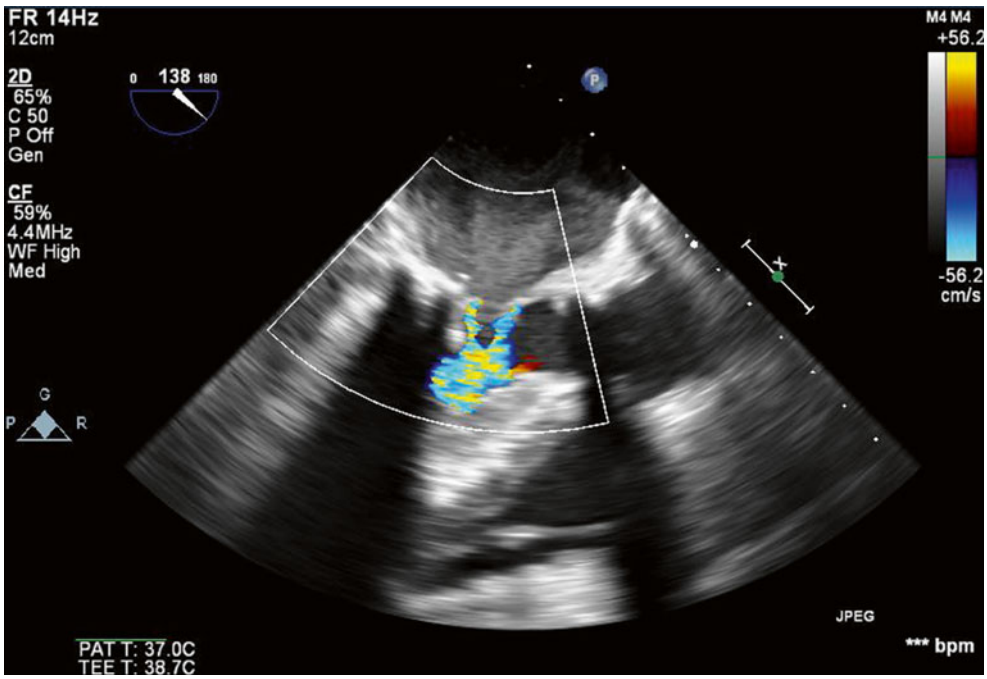

Fig. 11.65 Color Doppler imaging demonstrated only a small jet of turbulent forwards flow across the severely stenotic mitral valve

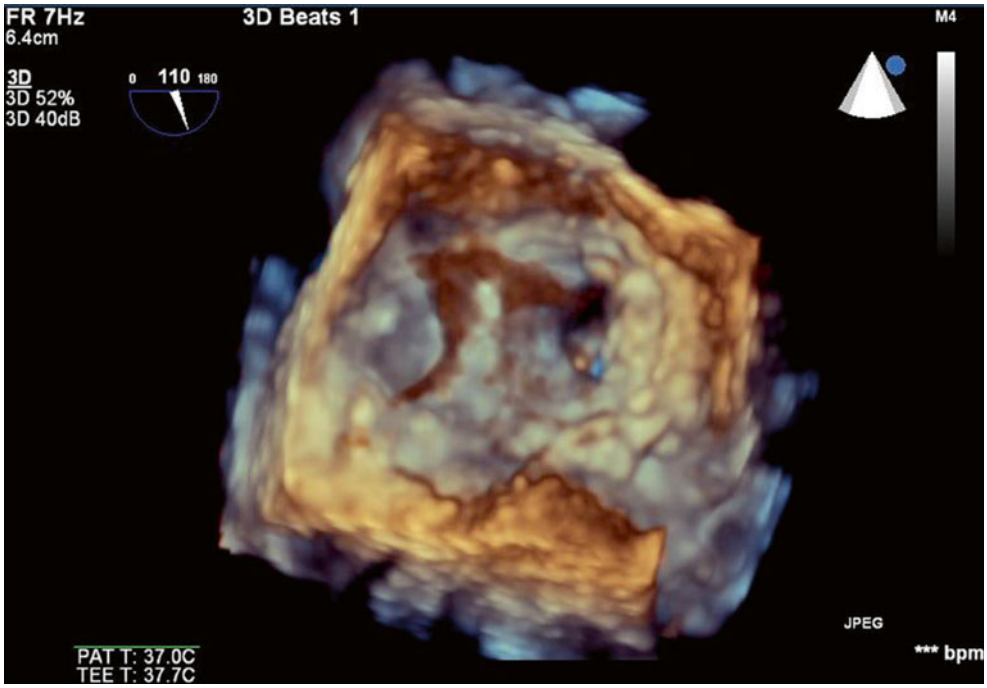

Fig. 11.66 3D reconstruction of the mitral valve showed a severely stenotic valve with only a slit-like valve orifice remaining

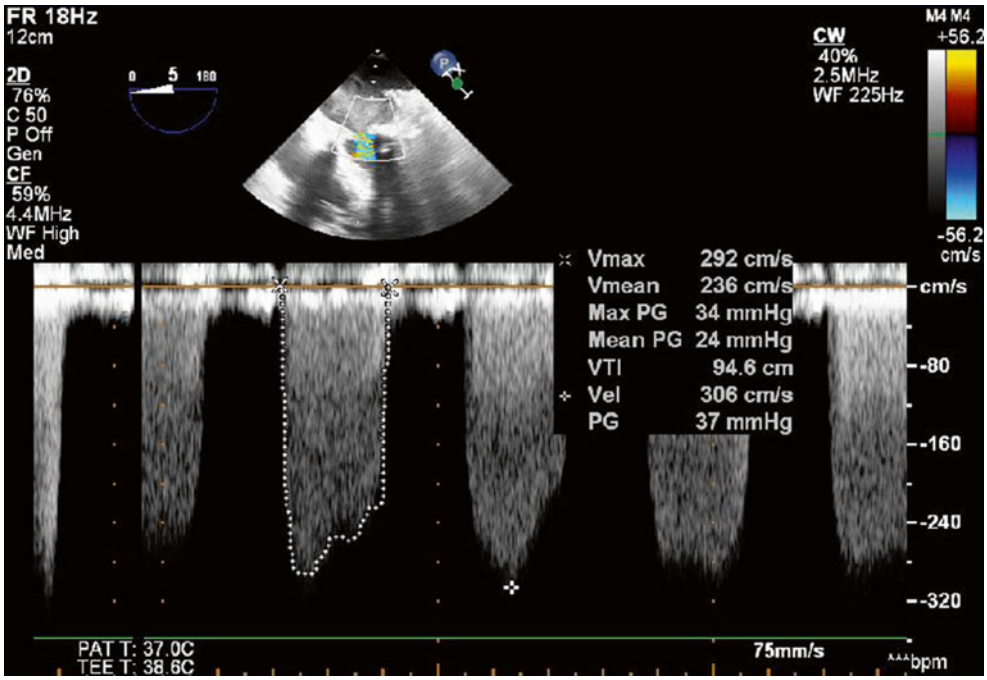

Fig. 11.67 Transvalvular gradients across the thrombosed valve had significantly increased to a peak and mean of 34 and 24 mmHg respectively

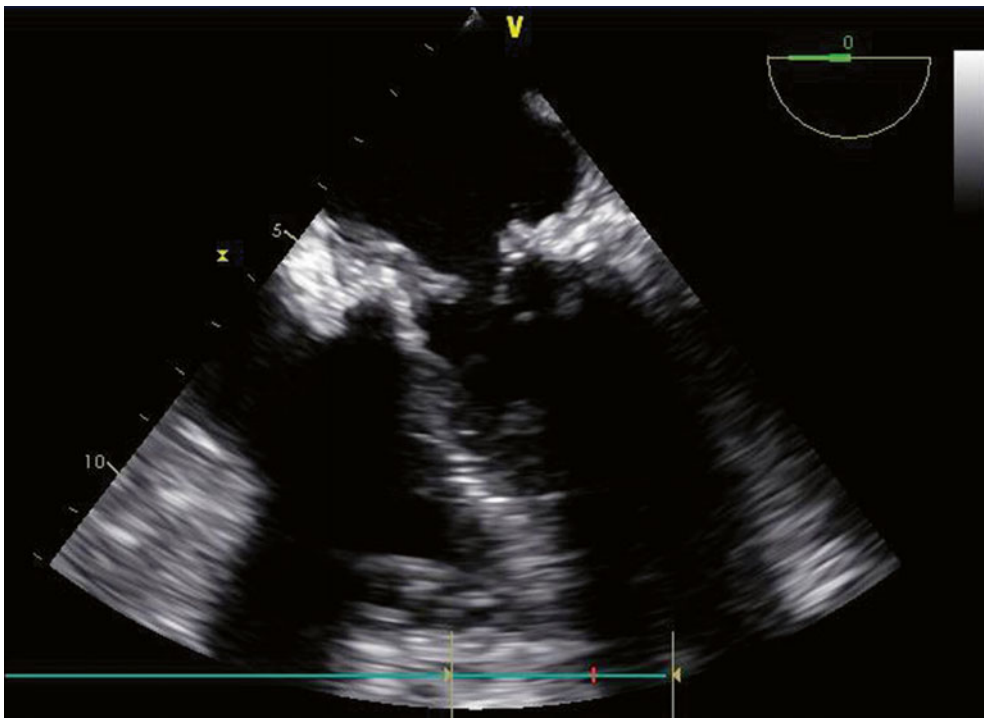

Fig. 11.68 After the thrombectomy, TEE (0° midesophageal view) demonstrated improved leaflet mobility, however a degree of restricted leaflet excursion persisted due to residual thrombus on the valve leaflets and annulus. Biventricular function remained severely impaired

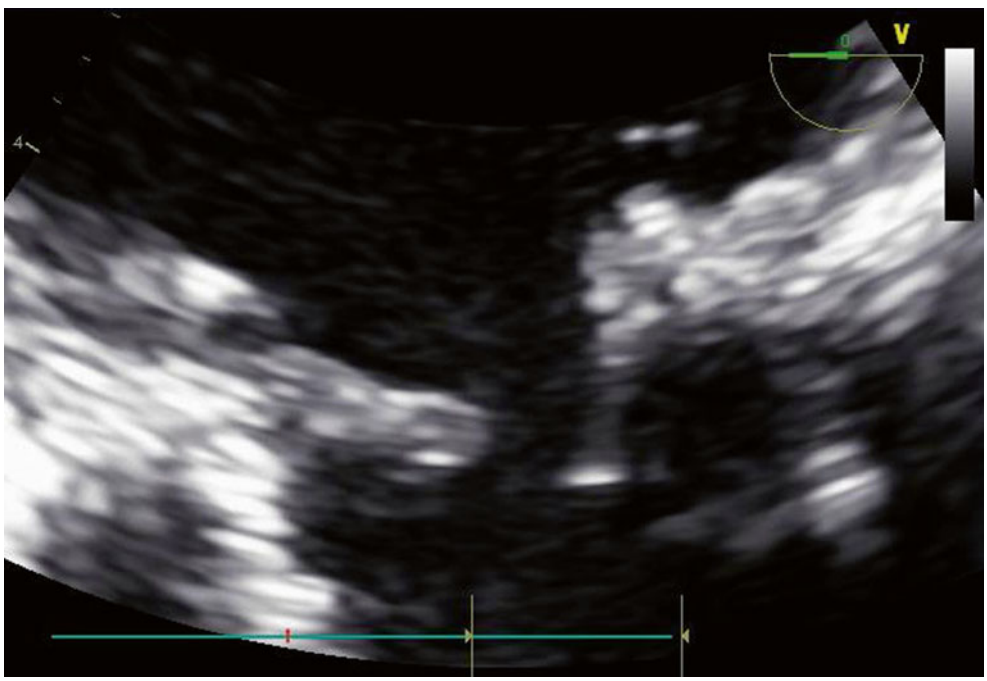

Fig. 11.69 Zoomed view of Fig. 11.68

11.13 Case 13. Mitral Valve Thrombus

A 77-year-old man with a past history of recurrent deep vein thromboses and an inferior vena cava filter presented with severe mitral regurgitation due to a partial flail anterior mitral valve leaflet. He underwent a mitral valve replacement with 31-mm Magna pericardial prosthesis. Several days later, he developed shortness of breath, congestion on chest x-ray, and atrial fibrillation.

Transesophageal echocardiography revealed layered thrombus measuring up to 1 cm in diameter within the left atrium, along the interatrial septum and within the left atrial appendage. The lateral leaflet of the mitral bioprosthesis was fixed and thickened, probably related to superimposed thrombus (Figs. 11.70, 11.71, 11.72, and 11.73).

The patient was found to have a complex hypercoagulable state related to lupus anticoagulant and heterozygosity for Factor V Leiden deficiency. He was maintained on therapeutic anticoagulation, with gradual reduction of the left atrial thrombus burden and improvement in symptoms. The lateral leaflet remained restricted, but given his hypercoagulable state, he was managed conservatively.

Video 11.60 (**a**) TEE (0° view) showing that the lateral prosthetic valve leaflet is relatively fixed because of overlying thrombus, which also extends onto the annulus (AVI 6167 kb)

Video 11.60 (**b**) Zoomed view of Video 11.60a (AVI 8609 kb)

Video 11.61 Color Doppler imaging demonstrated significant turbulence in the flow across the valve, suggestive of valvular stenosis. Trivial regurgitation was noted (AVI 2146 kb)

Video 11.62 3D imaging of the trileaflet, bioprosthetic mitral valve prosthesis viewed from the left atrium. Significant restriction of lateral leaflet is noted, with relatively preserved excursion of the other two leaflets (AVI 1227 kb)

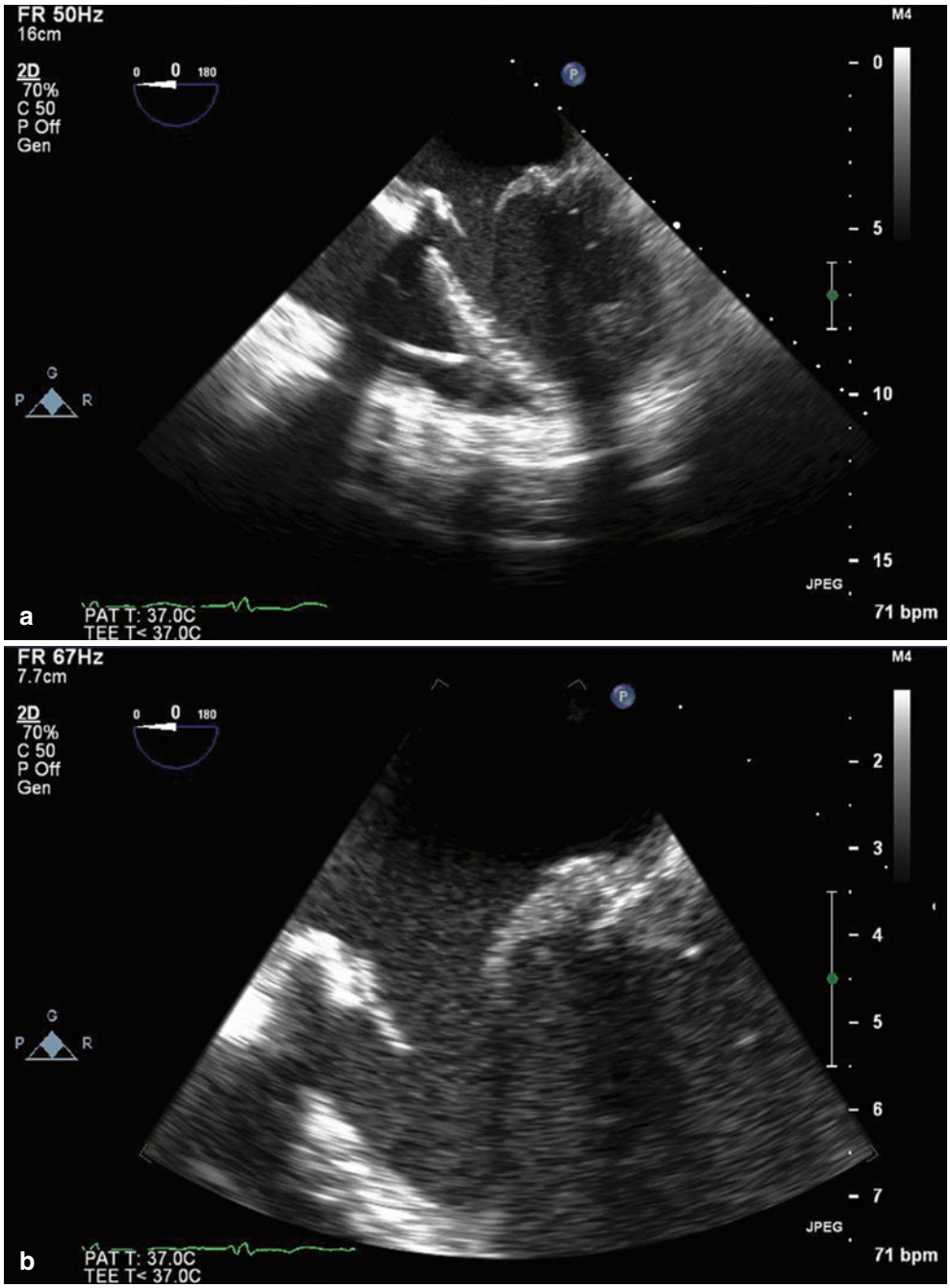

Fig. 11.70 (**a**) TEE (0° view) showing that the lateral prosthetic valve leaflet is relatively fixed because of overlying thrombus, which also extends onto the annulus. (**b**) Zoomed view

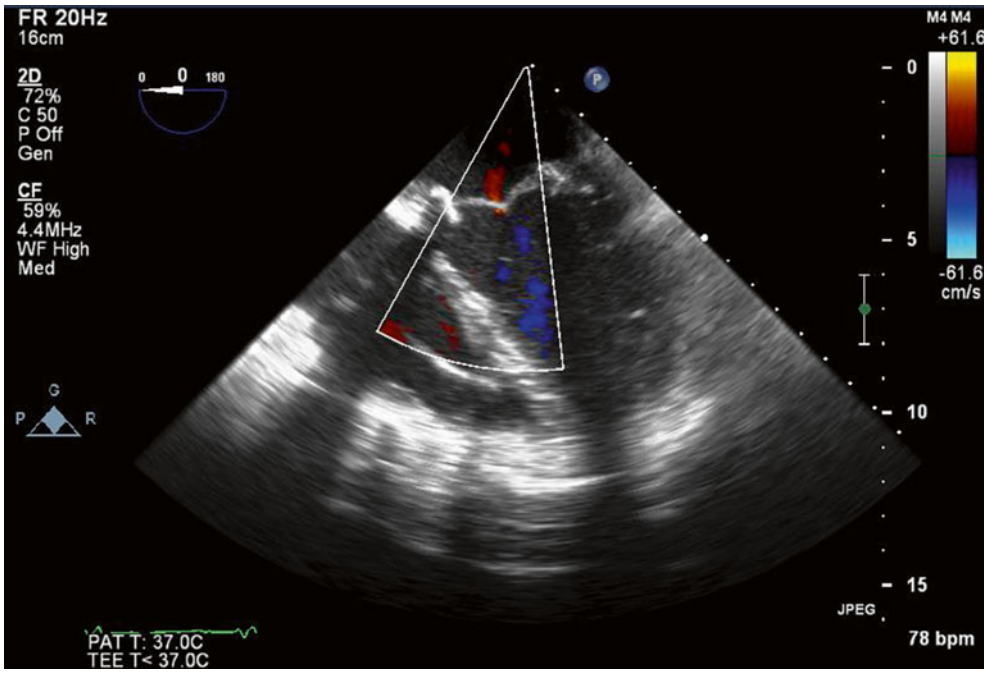

Fig. 11.71 Color Doppler imaging demonstrated significant turbulence in the flow across the valve, suggestive of valvular stenosis. Trivial regurgitation was noted

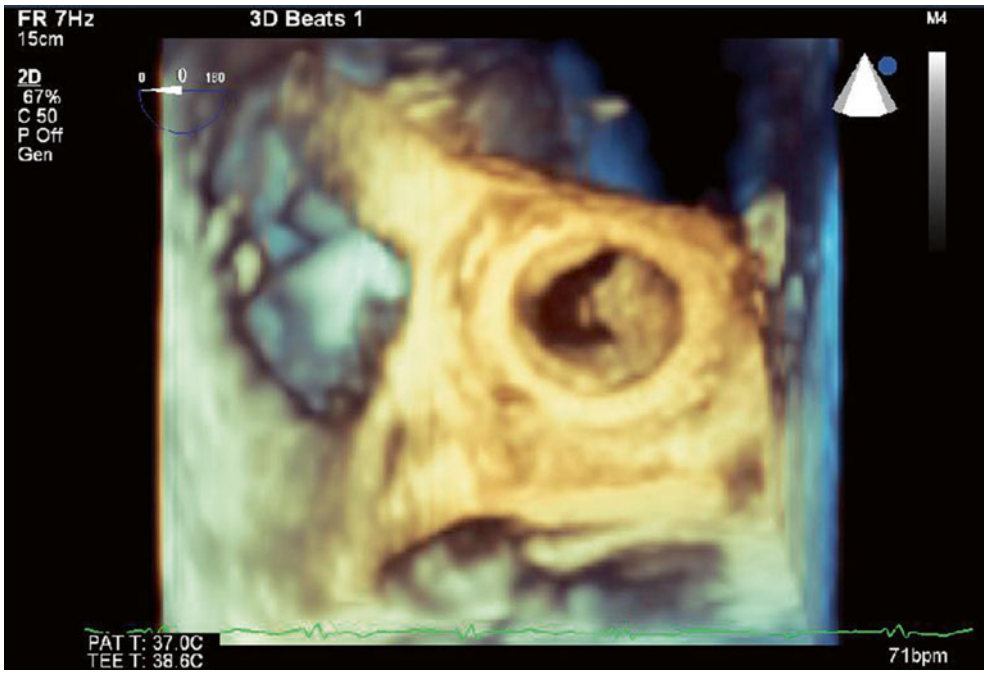

Fig. 11.72 3D imaging of the trileaflet, bioprosthetic mitral valve prosthesis viewed from the left atrium. Significant restriction of lateral leaflet is noted, with relatively preserved excursion of the other two leaflets

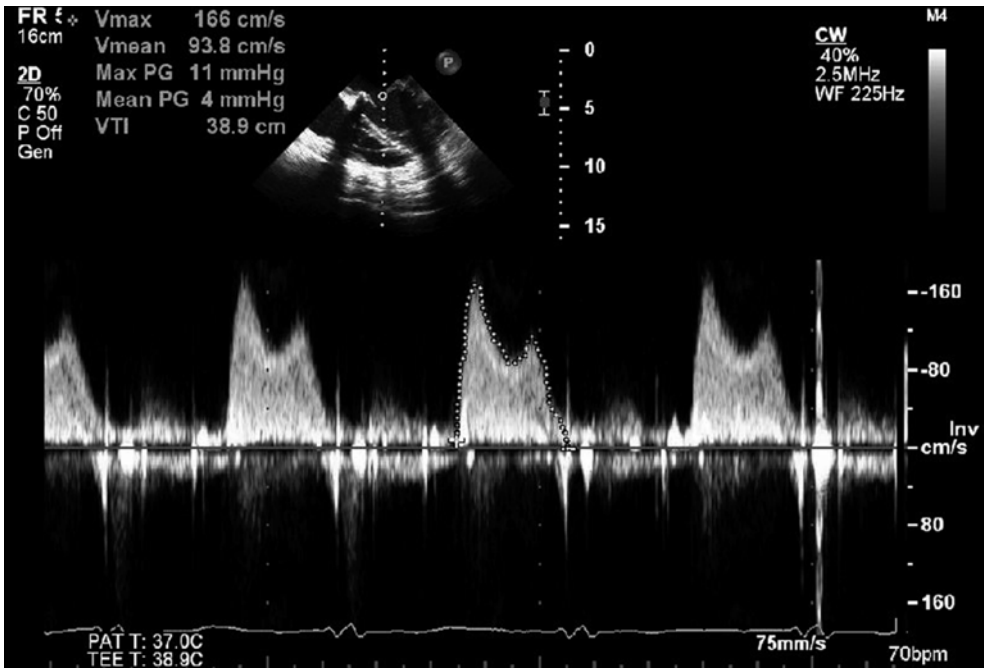

Fig. 11.73 Despite leaflet restriction, the transvalvular gradients were only mildly increased overall (peak, 11 mmHg; mean, 4 mmHg)

11.14 Teaching Points

- Hemolytic anemia in the setting of a paravalvular leak suggests that the defect is actually small. Turbulence of blood flow through the small communication results in hemolysis.
- Regardless of severity, the prognosis for ischemic mitral regurgitation is worse than for nonischemic mitral regurgitation. The recent changes in the AHA/ACC valve guidelines reflect this difference, reclassifying ischemic mitral regurgitation graded as 2+ and over as severe [1].
- Repair of the mitral valve is technically challenging. Overall, the highest rates of successful repair are achieved in valve centers of excellence by surgeons who perform high volumes of cases. A good replacement is always better than a poor repair, which may lead to premature redo surgery.
- A repair is usually preferred over a replacement because of both valve longevity and the avoidance of anticoagulation. Repair may not be feasible if the valve is stenotic, calcified, significantly thickened, or morphologically unsuitable. Valve surgery in the setting of ischemic mitral regurgitation remains controversial [2].
- Minimally invasive and percutaneous approaches for mitral valve surgery are gaining acceptance, although they lack long-term data regarding complication rates and durability. These approaches may be alternative treatment options for patients who are felt to be poor surgical candidates because of age or comorbidities.
- 3D/4D imaging has revolutionized our ability to diagnose and quantify prosthetic valve dysfunction [3].

References

1. Nishimura RA, Otto CM, Bonow RO, Carabello BA, Erwin 3rd JP, Guyton RA, et al. 2014 AHA/ACC guideline for the management of patients with Valvular Heart Disease: a report of the American College of Cardiology/American Heart Association Task Force on Practice Guidelines. Circulation. 2014;129:e521–643.
2. Kronzon I, Sugeng L, Perk G, Hirsh D, Weinert L, Garcia Fernandez MA, Lang RM. Real-time 3-dimensional transesophageal echocardiography in the evaluation of post-operative mitral annuloplasty ring and prosthetic valve dehiscence. J Am Coll Cardiol. 2009;53:1543–7.
3. Acker MA, Parides MK, Perrault LP, Moskowitz AJ, Gelijns AC, Voisine P, et al. Mitral-valve repair versus replacement for severe ischemic mitral regurgitation. N Engl J Med. 2014;370:23–32.